DYNAMICS OF PLATELET SHAPE CHANGE AND AGGREGATION IN SIZE-DEPENDENT PLATELET SUBPOPULATIONS.

by

© TRUMAN WONG

A Thesis submitted to the Faculty of Graduate Studies and Research in partial fulfillment of the requirements for the degree of Master of Science.

Department of Physiology
McGill University
Montreal, Quebec, Canada

AUGUST 1988

Truman Wong

Department of Physiology

M.Sc. Thesis short title:

Shape change and aggregation in size-dependent platelet subpopulations.

ABSTRACT

In mammalian species, platelets are heterogeneous with respect to many biochemical and functional characteristics. The functional significance of this heterogeneity is unresolved. To-date, studies of platelet aggregation have not focussed on the contributions of platelet mean volume (v), platelet number (N_o) and volume fraction ($\emptyset$) to aggregation responses. These parameters must be controlled in order to determine intrinsic platelet aggregability. Here, the relationship between v, N_o and platelet aggregation was evaluated in human platelet subpopulations separated by size using counterflow centrifugation. Micro-aggregation (PA) and macro-aggregation (TA) were determined respectively by electronic particle counting and turbidometry on the original platelet population and three size-dependent platelet fractions. At similar N_o, large platelets (L; v = 7.3±0.2 fl; 16±4% of the total population) were about two-fold more sensitive and more rapidly recruited into both micro (PA) and macro (TA) aggregates in response to ADP than the smallest platelets (S; v = 4.2±0.2 fl; 16±3%). At similar $\emptyset$, the above differences persisted solely for PA. In addition, maximal rates of shape change to ADP were the same for L and S platelets. Similar size-dependent results were obtained for platelet activating factor (PAF) and U46619, a thromboxane A_2 analogue, but no significant differences between L and S platelets were seen for ristocetin-induced agglutination. These distinct responses appear to arise from intrinsic biochemical differences present in size-dependent subpopulations for which a likely model is proposed.

RESUME

Chez les mammifères, les plaquettes sanguines sont hétérogènes en ce qui concerne de plusieurs caractéristiques biochimiques et fonctionelles. Sa signification fonctionelle demeure inconnue. Jusqu'à présent, les études sur l'aggrégation plaquettaire n'ont pas tenu compte de l'importance relatif de la grandeur moyenne plaquettaire (v), du nombre de plaquettes initial (N_o) et de la fraction de volume plaquettaire ($\emptyset$) aux réponses d'aggrégation. Ces paramètres doivent être controlées afin de connaître les capacités intrinsèques d'aggrégation des plaquettes. Dans l'étude présent, le rapport entre v, N_o et $\emptyset$ a été évalué pour des sous-populations plaquettaires humaines. Ces dernières étaient isolées selon leur grandeur par une centrifugation à contre-courant. La microaggrégation (PA) et la macroaggrégation des plaquettes (TA) ont été mésurées respectivement par comptage électronique des particules et par l'analyse de la transmission lumineuse des suspensions plaquettaires. Celles-ci ont été éffectuées sur la population plaquettaire complète et sur trois sous-fractions ayant de grandeurs distinctes. A N_o semblable, les grandes plaquettes (L;v = 7.3±0.2;soient 16±4 % de la population complète) étaient à peu près 2 fois plus sensibles et rapidement recrutées que les petites plaquettes (S; v = 4.2±0.2;16±4%) pour PA et TA induites par ADP. A $\emptyset$ semblable, les réponses ci-hauts mentionnés ont persisté uniquement pour PA. En plus, les taux maximales de changement de forme plaquettaire étaient les mêmes entre les plaquettes L et S. Des résultats semblables ont étés obtenus pour l'agent actionnant plaquettaire (AAP) et U46619, un analogue de thromboxane A_2, mais non pas pour l'agglutination induite par ristocetin. Ces réponses distinctes semblent provenir des caractéristiques

biochimiques et intrinsèques chez les sous-populations plaquettaires de différentes grandeurs, pour lesquels un modèle vraisemblable est proposé.

ACKNOWLEDGEMENTS

I wish to thank first of all, my research supervisor, Dr. M.M. Frojmovic. I am grateful for the many opportunities and privileges he has given me in the different capacities of our association. I thank him for his much devoted time and effort in reviewing this thesis. It has been a great experience to study under his guidance and authority.

My thanks as well to Drs. J. Milton and A. Wechsler for their encouragement and support.

To my colleagues of the lab from whom I received much assistance and friendly encouragement: F. Robert Lalla, Kimberley A. Longmire, Jane G. Wylie and in particular, Lloyd G. Pedvis; their friendships and fellowships made things easier throughout the course of this work.

I thank Fred Nestel, Emma Resurreccion and Drs. J. Mortola and C. Polosa for drawing blood from donors; Dr. B. Tuchweber and M. Audet of l'Université de Montréal for the use of the counterflow centrifuge; Margaret Eiteman for manuscript assistance.

Finally, I wish to dedicate this work to my family, for their patience and support.

Funding for this research was provided by grants from the Medical Research Council of Canada and the Fondation du Québec des maladies du coeur.

獻大給敬愛的父母親大人：

為你們始終不渝的支持幫助

理解和愛

PUBLICATIONS ARISING FROM THIS RESEARCH

Published Abstracts

Wong T, Frojmovic M M. Platelet size, not platelet mass, determines intrinsic kinetic differences in platelet recruitment into aggregates for ADP, U46619, and PAF, but not for ristocetin. Thrombosis and Haemostasis 1987:58;471.

Papers

Wong T, Pedvis L G, Frojmovic M M. Platelet size-dependent subpopulations: relative contributions of platelet number, volume fraction and biochemical differences to micro- and macro- aggregation for three physiological activators and for ristocetin. To be submitted in abbreviated form to Thrombosis Haemostasis.

TABLE OF CONTENTS

PAGE

PAGE

LIST OF FIGURES

PAGE

APPENDIX

LIST OF TABLES

CHAPTER II PAGE

APPENDIX

ABBREVIATIONS

AA	arachidonic acid
ACD-A	acid citrate dextrose, NIH formula A
ADP	adenosine diphosphate
AMP	adenosine monophosphate
ßTG	ß-thromboglobulin
C	control
Ca^{2+}	ionized calcium
cAMP	cyclic adenosine -3',5'-monophosphate
D	discocyte
DAG	1,2-diacylglycerol
DE	discoechinocyte
DTS	dense tubular system
e	optical density (extinction)
EDTA	ethylenediamine-tetraacetic acid
FBS	fibrinogen binding site
5HT	serotonin
Fn	fibrinogen
g	units of gravitational force
G_i	inhibitory G-protein
G_s	stimulatory G-protein
GP	glycoprotein
IP_3	inositol 1,4,5-triphosphate
k'	optical efficiency
L	large-sized
M	mid-sized
Mg^{2+}	ionized magnesium
MK	megakaryocyte
N	number of nuclear doublings
N_o	initial platelet particle count
N_t	platelet particle count at time t
PA	platelet microaggregation
PAmax	maximal extent of platelet microaggregation
PAF	platelet activating factor
PBS-A	phosphate buffered saline with 0.5% albumin
PDGF	platelet-derived growth factor
PF_4	platelet factor 4
PFP	platelet free plasma
PGE_2	prostaglandin E_2
PGG_2	prostaglandin G_2
PGH_2	prostaglandin H_2
PGI_2	prostaglandin I_2
ø	platelet volume fraction
PI	phosphoinositol
PIP	phosphoinositol-phosphate
PIP_2	phosphoinositol-diphosphate
PLA_2	phospholipase A_2
PLC	phospholipase C
PPP	platelet-poor plasma

PRP	platelet-rich plasma
r	linear correlation coefficient
r_p	axial ratio
S	small-sized
SC	shape change
SCCS	surface-connecting canalicular system
S.D.	standard deviation
SE	sphero-echinocyte
$t_{1/2}$	half-time
%T	percent light transmittance
%Tmax	maximal extent of macroaggrgation
$\%T_o$	initial percent light transmission
TA	platelet macroaggregation
TA-1	primary, reversible platelet macroaggregation
TA-2	secondary, stable platelet macroaggregation
TSP	thrombospondin
TXA_2	thromboxane A_2
U46619	a stable PGH_2/TXA_2 analogue
v	mean platelet volume
V_a	rate of platelet aggregation (from %T)
vol	volumes
V_s	rate of platelet shape change (from %T)
vWf	von Willebrand factor
WB	whole blood
ZK 36374	a stable PGI_2 analogue

CHAPTER I.

GENERAL INTRODUCTION

1.- THE IMPORTANCE OF PLATELETS IN HEMOSTASIS.

Platelets play a central role in both physiological hemostasis and pathological thrombosis. Although platelets occupy a small relative volume fraction of circulating blood, (< 0.2% v/v), they are critically needed for arresting blood loss and restoring vascular integrity following trauma [1-4]. In thrombosis, platelets often participate in pathological mechanisms which induce damage and/or tend to subsequently occlude the vasculature.

In the non-activated state, platelets circulate as elliptical, disc shaped cells, moving in close proximity to and thus often colliding with the luminal side of blood vessels [5]. Normally, platelets do not adhere to a morphologically intact and healthy endothelial wall. However, endothelial injury (arising from trauma or pathology) can expose subendothelial materials such as collagen, elastin, and microfibrils, whose reactions with blood activates the hemostatic mechanism. Platelets colliding with the newly exposed materials are activated upon contact. Platelets undergo a quick morphological change from that of the smooth discoid to a more spheroid form. This is followed by their adherence to the exposed subendothelium as well as their adherence to each other, i.e., aggregation [1,5].

Activated platelets can release factors which induce further activation of nearby platelets in circulation. Substances such as ADP, thrombin and adrenalin induce platelet aggregation which will form a platelet plug at the site of injury. Thus, the activities of platelets can be generally described in stepwise fashion:

(1) adhesion: sticking to and spreading onto exposed endothelium or foreign surfaces.

(2) aggregation: adhesion of platelets to one another, initially forming aggregates of < 10 platelets, followed by build-up of much larger aggregates (> 100's of platelets) from the smaller sized aggregates.

(3) secretion: active release of stored granular contents following activation which stabilizes large aggregates [6].

(4) procoagulant activity: coagulation occurs in response to injury or under pathological conditions and platelet surface properties accelerate the reactions leading to the formation of fibrin.

(5) clot retraction: platelets are required for contracting a platelet-fibrin meshwork into a more tightly packed, less hydrated clot with enhanced mechanical strength. This is related to clot consolidation, mediated by the contractile activity of fibrin-bound platelets [3].

2. - PLATELET STRUCTURAL ANATOMY

Under resting conditions, platelets circulate as disc-shaped, anucleated cells, called discocytes (D) [1,5]. Close examination of platelets under electron microscopy reveals surface indentations and a general roughness which represent sites of exchange between channels of the surface connected canalicular system (SCCS) and the exterior environment [7]. The SCCS constitute the portion of plasma membrane that is invaginated. This type of surface connection found in the outer membrane is exclusive to platelets and is not found in any other blood cell type. Under light or phase contrast

microscopy, the internal structure of the platelet appears simple and cannot be studied in great detail. Fine examination of platelet internal structure has also required the use of electron microscopy. To facilitate the relationship between structure and function, White and Gerrard [8] have devised a useful classification that divides platelet structure into 4 main regions (refer to Figure 1).

(1) The peripheral zone is the outer region consisting of the membranes and closely related structures forming the platelet surface and the convoluted channels of the SCCS. Since channels of the SCCS represent invaginations of the cell wall, the peripheral zone is a continuous structure. This zone can be further divided into 3 components: the exterior coat, the unit membrane, and the submembrane region. The exterior coat, also known as the glycocalyx, is thicker and denser than the surface coats of other blood cells. The glycocalyx is a lining 150 to 200 Å thick and rich in glycoprotein content. There are at least 8 different glycoproteins types which make up the glycocalyx. Some of these are exclusive to platelets and are specifically involved in generation of platelet stickiness and subsequent adhesion or aggregation. The receptors for agonists that elicit platelet activation, and for adhesive proteins mediating adhesion/aggregation reactions, are also found in this exterior coat.

The platelet unit membrane resides in the peripheral zone and acts as barrier between intracellular and extracellular components. The intermediate layer of the peripheral zone contains a high proportion of phospholipids which play a critical role in providing a surface for

Figure 1. Diagram of an edge-on discoid platelet in cross section as it would appear in electron microscopy. Components of (1) the peripheral zone include: the exterior coat (E.C.), trilaminar unit membrane (C.M.), dense bodies (D.B.); (2) the sol-gel zone: microtubules (M.T.) and glycogen (Gly); (3) the organelle zone: mitochondria (M); granules (G); and dense bodies (D.B.). (From: White J G and Gerrard J G. Anatomy and structural organization of the platelet. In: Hemostasis and Thrombosis. J B Lippincott, Toronto 1982.)

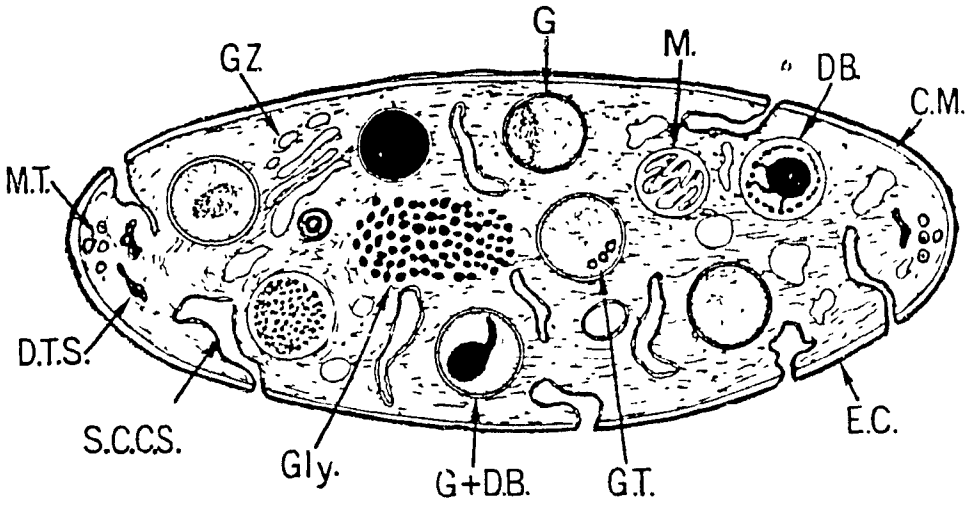

interaction with plasma coagulant proteins. The last and innermost layer of the peripheral zone serves to transmit signals received from the outside surface into secondary messages required for further platelet activation. These secondary messengers may be in the form of a biochemical intermediate or a physical alteration of the membrane constituents.

A system of filaments physically similar to microfilaments of microtubules is found here. These submembrane filaments interact with the circumferential microtubules of the sol-gel zone (described below), to help maintain the discoid shape of the platelet. In addition, they may also play a role in pseudopod formation and interact with other components of the platelet contractile mechanism to carry out platelet aggregation and clot retraction as well.

(2) The sol-gel zone consists of the matrix of the platelet cytoplasm. It also contains structural proteins which enable the platelet to assume a discoid shape under resting conditions. The two major protein types found in this zone are the microfilaments and a circumferential band of microtubules. More importantly, actin and/or myosin proteins in this region provide a contractile system which mediates shape change, pseudopod expression and secretion following appropriate stimuli. The discoid shape is primarily attributed to a polymerized state of tubulin, a major protein component of microtubules. The location of the circumferential band of microtubules along the cross sectional plane underneath the cell wall in discoid-shaped platelets is suggestive of its importance in cytoskeletal support. Loss of the discoid form is associated with the contraction of this circumferential band. Contractile activity that is typically induced by physiological

activators is associated with central movement and constriction of the microtubules.

(3) The organelle zone is that region of the cytoplasm where granules, electron dense bodies, lysosomes and mitochondrion are randomly found. These organelles are involved in platelet metabolic processes, storage of enzymes and other vital components such as serotonin and calcium. There are also storage granules which are discharged of their products during platelet secretion. Three types of granules are found in platelets: dense granules, α-granules and acid hydrolase lysosomes. These organelles are heterogeneous with respect to differences in their size, density of their content as seen under electron microscopy and to the degree of microtubule association.

With an appropriate stimulus, the contents of these organelles are selectively expelled to the exterior environment without any simultaneous loss of material from other subcellular compartments. Platelet secretion occurs via fusion of organelles with the SCCS channels which provide a conduit for granular contents to the cell exterior.

(4) The dense tubular system (DTS) is a membrane system that falls in a grey area with respect to the above divisions. Channels here are distinguished from the clearer appearance of the SCCS channels. The DTS may participate in stabilizing the circumferential microtubules in the maintenance of platelet discoid shape [9]. More notably, this system is the site of sequestration for calcium, important for initiating contractile activity. Both intracellularly stored calcium and the presence of a Ca^{2+}, Mg^{2+} -ATPase found here regulate intracellular calcium fluxes and platelet activity in general. It also contains the enzymes necessary for the synthesis of prostaglandins (endoperoxides and thromboxanes)

during platelet activation. The SCCS, in close proximity with the DTS, provides access of products from the DTS to the exterior of the platelet.

3.- PLATELET GLYCOPROTEINS

The responses of platelets to stimulating agents are usually mediated by the platelet plasma membrane since these agents are excluded from the cell. This membrane has receptors for these agents and must transit signals arising from stimulus-receptor interactions [10,11]. The platelet plasma membrane consists of a layer that is 100 Å to 150 Å thick, the glycocalyx, which extends about 150 Å from the membrane surface. The platelet membrane is composed of ~10% carbohydrate, ~40% protein, and ~50% lipid [12]. Since sugar residues are attached to some lipids or proteins, the membrane also contains glycolipids and glycoproteins. With the exception of the two contractile proteins, actin and myosin, most proteins found in or associated with the platelet plasma membrane are glycoproteins. For example, glycoproteins can link surface bound substrates with the internal contractile system. This occurs when inner portions of either GP Ib or GP IIb-IIIa associate with actin-binding protein or actin filaments.

Platelet glycoproteins may act as receptors for agents that elicit activation or inhibit function [10,11,13]. Glycoproteins mediate pro-coagulant activity by interacting with coagulant proteins (i.e. intrinsic/extrinsic pathway clotting factors) which lead to fibrin formation. The receptors for some high molecular weight proteins such as von Willebrand factor (vWf) and fibrinogen (Fn) can be expressed on the platelet surface, enabling platelet adhesion and aggregation. One class of receptors, cytoadhesins, which are modified glycoprotein IIb-IIIa, bind

Fn and vWf in mediating respectively, interplatelet aggregation and adhesion onto subendothelium [14]. Considering the vital functions of glycoproteins in adhesion and aggregation, it is not surprising that several bleeding disorders (e.g., Glanzmann's thrombasthenia, Bernard-Soulier syndrome) are caused by deficient or defective platelet glycoproteins [13,15].

3 (i) GLYCOPROTEIN CLASSIFICATION.

Both membrane proteins and glycoproteins can be divided into two categories depending on the nature of their attachment to the membrane. Peripheral proteins are bound to only the outside bilayer of the membrane whereas integral proteins are usually transmembrane and therefore more tightly bound (see Figure 2). The arrangements of proteins and glycoproteins are asymmetric, with some portions of the glycoproteins extending beyond the outside of the membrane. Sialic acid residues are part of the glycoprotein structure, thus contributing to the negative charge of the membrane [10]. Glycoproteins were originally classified using Roman numerals (e.g., I, II) in order of decreasing molecular size [16]. Finer divisions were subsequently made possible with improved labelling techniques [17,18]. The nomenclature was expanded by using the above numerical designations along with an additional letter to assign glycoproteins within the similar molecular weight class (e.g., glycoprotein Ia, glycoprotein Ib).

Figure 2. The various types and orientations of platelet membrane glycoproteins. Numerals and lettering denote the glycoprotein species. The interaction of glycoprotein with contractile actin filaments is depicted. (From: Phillips D R. Platelet membranes and receptor function. In: Hemostasis and Thrombosis. J B Lippincott, Toronto 1982.)

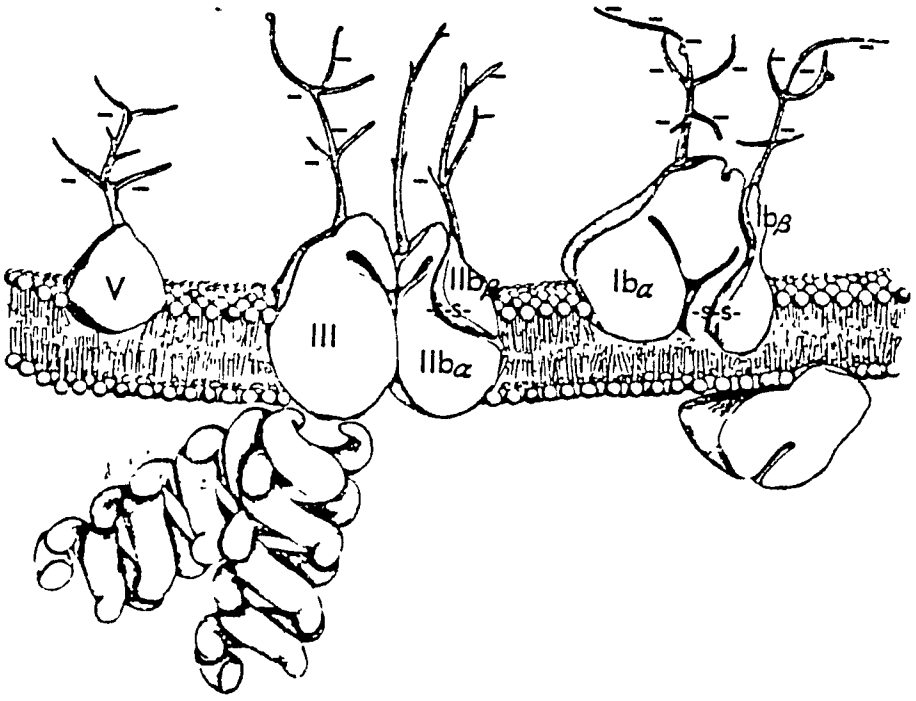

3 (ii) GLYCOPROTEIN IIb-IIIa

Glycoproteins IIb and IIIa, each at about 75,000 per platelet, are the two most common glycoproteins found in platelet membranes [11,13]. The two glycoproteins together form a single, calcium-dependent, heterodimer complex (GP IIb-IIIa) that can act as the receptor for fibrinogen mediated platelet aggregation. About two-thirds of the complexes are randomly dispersed on the platelet surface, while the remainder are found between membranes of the SCCS and the α-granules. Regardless of their location at rest, all complexes are likely accessible on the surface of activated platelets. The topical complexes are transmembrane and may interact with actin filaments within the platelet under stimulus conditions.

GP IIb-IIIa complexes undergo conformational changes on the membrane surface to acquire the ability to bind fibrinogen [19]. Structural changes appear to be a prerequisite in binding to adhesive proteins. There is also evidence to suggest that Fn, when bound to GP IIb-IIIa, interacts with thrombospondin (TSP) in adhesive reactions [20]. TSP is an alpha granule protein that is secreted upon platelet stimulation and is believed to have GP IV as its receptor [21]. The interaction with TSP appears to stabilize fibrinogen binding to GP IIb-IIIa, thus strengthening platelet-platelet linkage. Studies have also suggested the ability of GP IIb-IIIa to bind other adhesive proteins, namely vWf and fibronectin [22,23].

Cellular redistribution of GP IIb-IIIa occurs during platelet stimulation. Interaction with adhesive proteins leads to clustering and localization of these complexes at platelet pseudopods and at regions of inter-platelet contact [22]. In addition, adhesive proteins (vWf, Fn and fibronectin) are localized on the platelet surface following

their release from intracellular granules [24]. Whether activated by weak or strong agonists, platelets change shape and express fibrinogen binding sites on their membrane surfaces. Fibrinogen binding is normally a prerequisite for aggregation and is dependent upon the GP IIb-IIIa complex. Amongst all adhesive proteins, Fn appears most preferentially used as a cross linking agent in platelet-platelet cross-linkage [11,25].

4. FUNCTIONAL EXPRESSION IN PLATELETS.

4 (i) PLATELET SHAPE CHANGE.

Activation of platelets by a variety of agonists leads to morphological changes on the platelet body (Figure 3) [1, 5, 26]. The shape change occurs following the interaction of activators such as adenosine diphosphate (ADP) with specific receptors present on the plasma membrane. The morphological changes are due to biochemical and physical mechanisms in the platelet that alter its shape. Changes in platelet size and surface topology of the platelet membrane are reflective of shape change. These changes can also be induced following adhesion to reactive materials such as collagen. Many platelet functional expressions such as adhesion, aggregation and release are associated with changes in its structure.

The extent of platelet shape change depends on the activator type and strength of the stimulus, as well as the time elapsed following activation. An unactivated discocyte (D) undergoes changes whereby it loses its smooth discoid shape to become more spherical and thus its axial ratio (r_p = t/d = thickness (t) over diameter (d)) increases. The surface membrane becomes more ruffled with an apparent increase in roughness, thin projections called pseudopods

emerge from the main body, and there is a net increase in platelet size.

These changes have been collectively referred to as a hypervolumetric shape change [5], and may be associated with an increase in externalized plasma membrane. The source of this extra surface membrane may derive from SCCS membranes. At this point, the platelet is called a disco-echinocyte (DE), see Figure 3, which depicts discocyte-echinocyte transformations. The DE term reflects the presence of pseudopods and the sustained ellipsoid shape of the platelet. The transformation from D to DE is initiated within ~100 milliseconds of activation [26], with maximal conversion by 8 - 10 seconds [5]. Under appropriate stimulus conditions, the DE undergoes further changes to become a sphero-echinocyte (SE). The latter is characterized by a spherical body, highly ruffled surface membrane and optimally long pseudopods (1-3 μm).

This classification of platelet morphology is largely based on the appearance of platelets under phase contrast microscopy (Figure 4) [5]. Under these conditions, discocytes appear as clear ellipsoids edge on ($r_p < .5$), while face on they appear round and dark throughout. Sphero-echinocytes under any orientation appear circular ($r_p > .9$) with a clear center and relatively prominent pseudopods. Disco-echinocytes are those platelets which do not meet the criteria set for D and SE. These are convenient terms to categorize platelet shape, bearing in mind however, that there is a continuous spectrum of shapes ranging from the smooth D to the spherical, pseudopoded SE.

Platelet shape change has been studied using various microscopy techniques such as phase contrast, interference contrast and transmission electron microscopy [5, 27, 28]. These studies have arrived at a common agreement that platelets assume different shapes adequately defined by the D, DE and SE classification.

Figure 3. The sequence of platelet shape change associated with platelet activation. Morphological changes from unactivated discocyte (D) --> disco-echinocyte (DE) --> sphero-echinocyte (SE) can be reversible. (From: Frojmovic M M and Milton J G. Blood Cells 1983:9;360.)

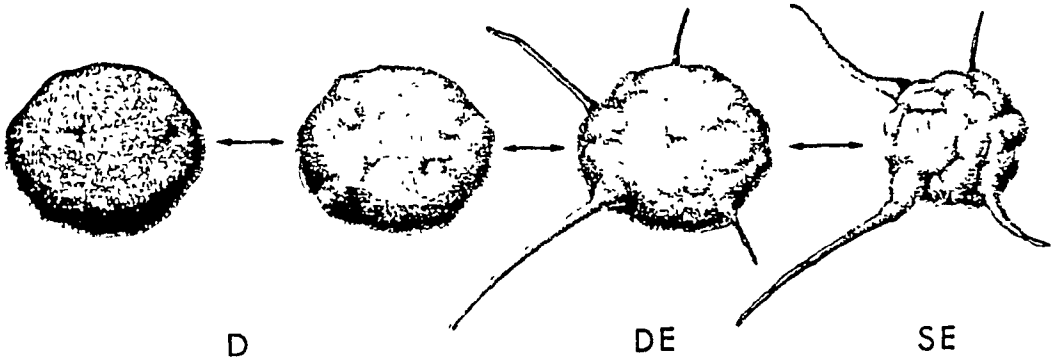

Figure 4. Typical examples of discocytes, disco-echinocytes and sphero-echinocytes as viewed under phase contrast microscopy. A,B: face-on and edge on view of a discocyte; C, D, E: disco-echinocytes with increasing roundness towards sphero-echinocyte; and F: sphero-echinocyte. Final magnification 3000x (From Frojmovic M M and Milton J G. Physiol Rev 1982:62;187)

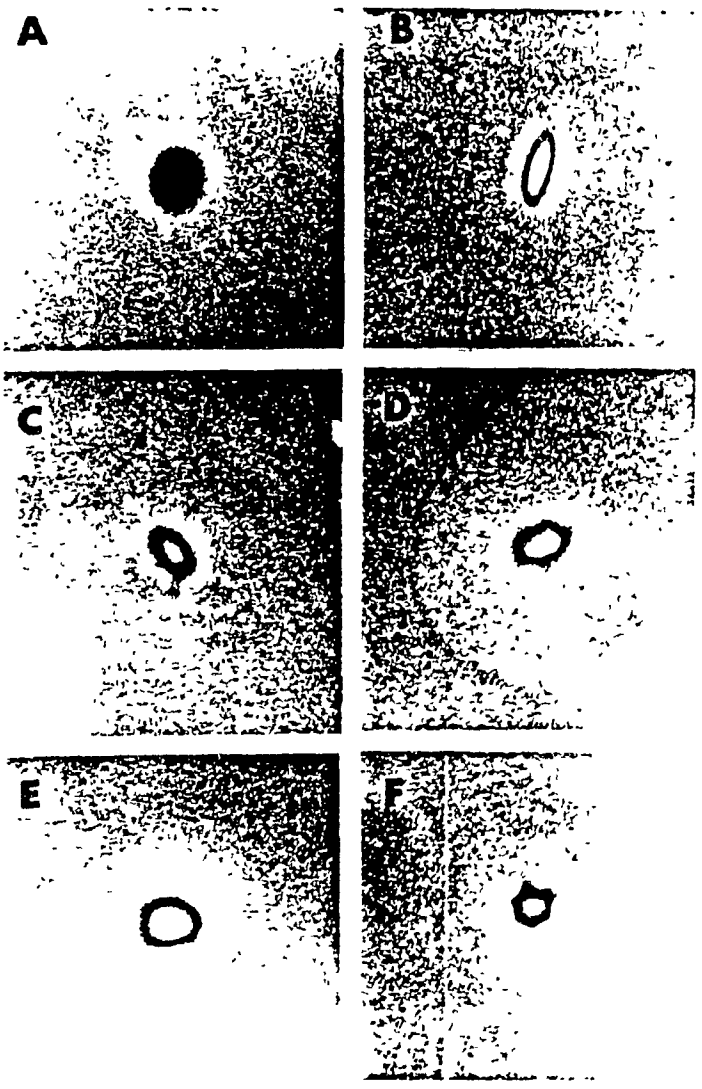

Another method used to study shape change is aggregometry, which monitors changes in light transmission of a suspension of platelet-rich plasma (PRP) following addition of an agonist [27]. A certain portion of the aggregometry tracing is deemed to reflect shape change. This portion corresponds to the initial decrease in % light transmission (%T) following activator addition. Changes in platelet axial ratio, mean volume, refractive index and pseudopod formation all contribute to the changes in %T. While platelet volume increase and pseudopod projection both tend to increase %T, changes in platelet axial ratio (toward 1) and refractive index diminish %T. Refractive index may be altered due to: 1) influx or efflux of water ; 2) externalization of invaginated membrane (i.e., SCCS membranes) and 3) changes in membrane intrinsic properties. It is uncertain whether changes in refractive index directly parallel shape change. However, it has been shown that the initial decrease in light transmission occurring with turbidometrically measured activation does reflect the initial rate of D to DE transformation [27]. The initial rate of %T decrease essentially reflects changes in platelet axial ratio, with more minor contributions due to pseudopod formation in the first few seconds of shape change. These observations have been confirmed by parallel microscopic studies [27-29].

Analyses using both microscopy and aggregometry can describe shape change in terms of rates and extents. For example, measurements of initial decreases in turbidity of platelet suspensions following agonist addition have kinetically described platelet shape change [30]. This kinetic measure of shape change would reflect biochemical and functional properties of platelets as described above. Morphometric measurements of shape change support aggregometric measurements of shape change, and have indicated that D are transformed to DE bearing 1 to 3

pseudopods per platelet within about 8 to 10 seconds post activation. DE formation is accompanied by an increase in cell volume of ~40%. This is followed by SE formation, detectable by ~8 to 10 seconds, reaching a maximum by ~15 seconds, and accompanied by a ~20% decrease in volume in comparison to the original unactivated D [5,29].

Internal platelet rearrangements occur with shape change. Loss of discoid shape along with pseudopod projection are associated with cytoskeletal re-organization [8]. The intracellular organelles centralize, micro-tubules partially dissociate, and contractile proteins are re-organized. Specifically, the circumferential band of microtubules, along with contractile proteins actin and myosin, assemble into highly organized structures that contract centrally and thereby converging storage granules in the cell center. Myosin-actin interactions generate the forces required for subsequent release who can occur following these internal events [31]. These intracellular events are necessary for the generation of adhesiveness on the surface membrane, priming the platelets for subsequent aggregation, as well as for the induction of pro-coagulant activity.

4 (ii) THE ROLE OF SHAPE CHANGE IN AGGREGATION.

In the presence of extracellular calcium and fibrinogen, shape changed platelets can be recruited into micro-aggregates (PA). It has been shown that shape change is a necessary requirement for early aggregation induced by the platelet agonists, adenosine diphosphate (ADP) and adrenaline [29]. Shape-changed platelets are preferentially recruited into early aggregates of ~10 platelets. Pseudopod formation, in particular, appears to be crucial in allowing aggregation to occur. It has been shown that pseudopods can

be formed in the absence of any significant changes in r_p or main body volume for adrenaline used as activator [5]. The latter two parameters appear to be less important in early aggregation. Platelet sphering is likely to be more important in the advanced stages of aggregation associated with secretion.

The presence of pseudopods is expected to favor platelet aggregation by reducing electrostatic repulsions between platelets and by increasing platelet collision frequencies due to increased collision diameter [1,32]. Furthermore, these projections can increase the surface area of cell-cell contact, thereby stabilizing adhesion [33].

Finally, there is evidence indicating that following activation, adhesive proteins and their respective glycoprotein complexes are localized on pseudopods between adjacently adhered platelets [20].

4 (iii) INTRACELLULAR SIGNALS IN ACTIVATION.

The morphological changes observed with platelet activation parallel important biochemical events occuring intracellularly. These biochemical reactions can be categorized as those that lead to either 1) an alteration in structure, i.e., shape change or 2) expression of other functions, i.e., adhesion and secretion. It is believed that following platelet-agonist interaction, movements of Ca^{2+} from outside the platelet through the plasma membrane and/or from the intracellular dense tubule system to the cytoplasm constitute the final pathway for activation [34, 35].

Two major pathways lead to calcium mobilization (Figure 5): one centered on Ca^{2+} movement from intracellular stores, the other centered on diacylglycerol (DAG) formation and associated protein phosphorylation [36]. Movement of Ca^{2+} during activation derives from 1) external Ca^{2+} moving into

the platelet interior; 2) Ca^{2+} released from DTS sites and 3) dense granule release of stored Ca^{2+}.

Ca^{2+} movements and intracellular activation depend on the generation of two intracellular messengers: 1,2-diacylglycerol (DAG) and inositol 1,4,5-triphosphate (IP_3), both of which depend on receptor-mediated activation of phospholipase C (PLC) [36,37]. DAG leads to protein kinase C activation, protein phosphorylation and non Ca^{2+} dependent activation while IP_3 can mobilize Ca^{2+} from intracellular stores.

Following IP_3 generation, freed Ca^{2+} activates enzymes such as phospholipase A_2 which lead to the generation of thromboxane A_2 (TXA_2) from arachidonic acid. TXA_2, in addition to direct mobilization of Ca^{2+} stores, can activate PLC which renders more IP_3 and DAG. The further production of these two intermediates provides the greatest amplification of Ca^{2+} movements which are important intracellular events leading to, or associated with platelet shape change, aggregation and release.

Ionized calcium functions as a second messenger for other intracellular reactions associated with stimulus-response activity [38]. These include microtubule depolymerization, actin-myosin contraction and mobilization of phospholipase A_2 . The ability to regulate Ca^{2+} would also control the activity level of the platelet. For example, the maintenance of discoid shape would depend on modulating intracellular Ca^{2+} concentrations, and may involve an intermediate such as cyclic AMP which inhibits Ca^{2+} mobilization.

The concentration of intracellular Ca^{2+} can coincide with the level of activation [39]. Relatively low Ca^{2+} concentrations have been reported during shape change whereas higher concentrations appear associated with further stages of activation, i.e., shape change --> micro-aggregation --> macroaggregation --> stable macro-

Figure 5. Platelet biochemical pathways associated with Ca^{2+} and intracellular signals following activation. Of central importance are the involvement of inositol tri-phosphate (IP_3) and diacylglycerol (DAG) with the endoperoxide pathway generating thromboxane A_2 (TXA_2). For definitions of abbreviations, see p. xiii . (From: Longmire K A. MSc. Thesis, p.47, McGill University, Montreal 1988). Figure shown on next page.

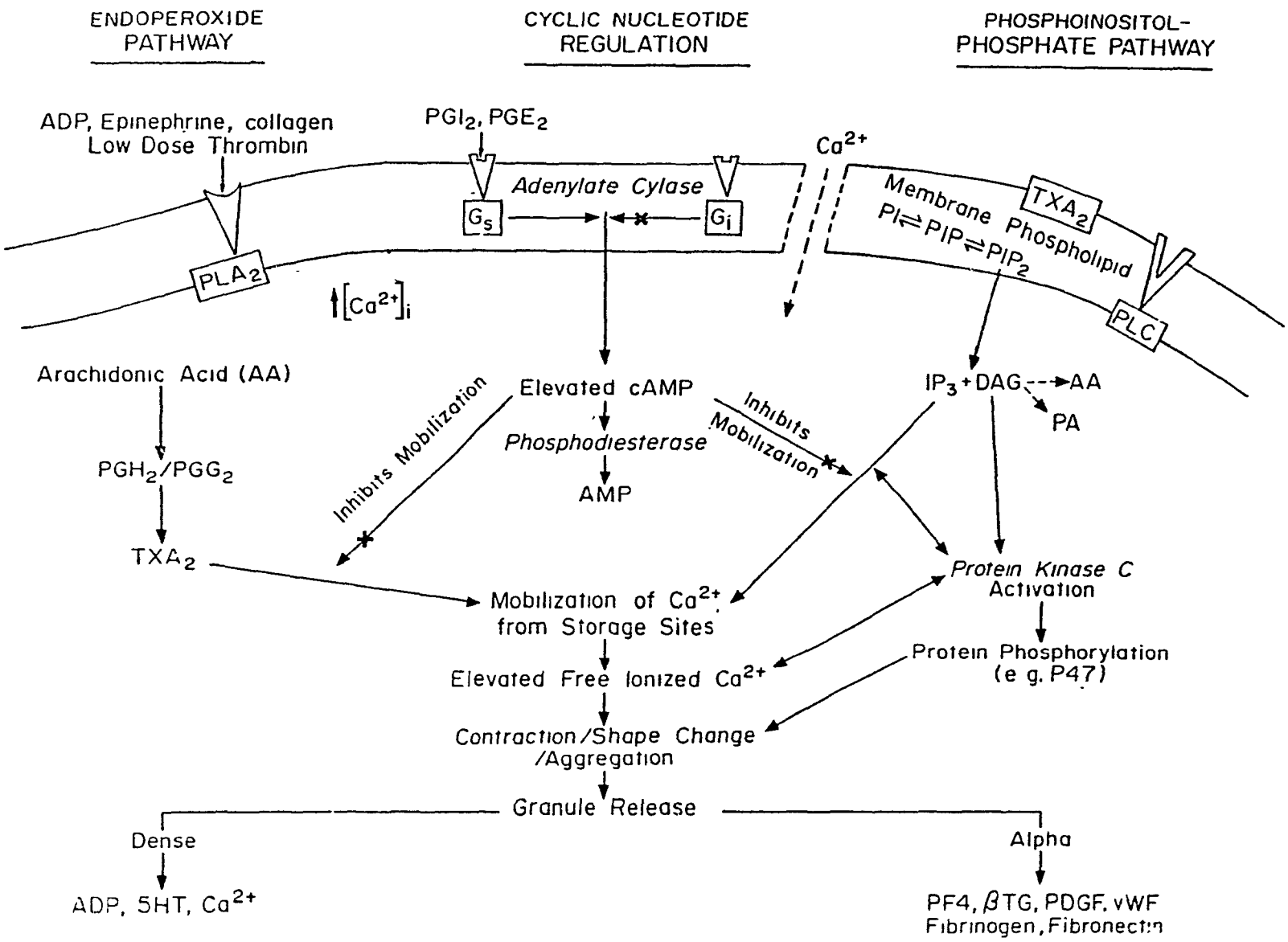
ENDOPEROXIDE PATHWAY
CYCLIC NUCLEOTIDE REGULATION
PHOSPHOINOSITOL-PHOSPHATE PATHWAY
ADP, Epinephrine, collagen Low Dose Thrombin
PGI2, PGE2
Ca2+
Adenylate Cylase
Gs
Gi
Membrane Phospholipid
PI⇌PIP⇌PIP2
TXA2
PLA2
↑[Ca2+]i
PLC
Arachidonic Acid (AA)
Elevated cAMP
IP3 + DAG
AA
PA
Inhibits Mobilization
Phosphodiesterase
Inhibits Mobilization
AMP
PGH2/PGG2
TXA2
Protein Kinase C Activation
Mobilization of Ca2+ from Storage Sites
Protein Phosphorylation (e g. P47)
Elevated Free Ionized Ca2+
Contraction/Shape Change /Aggregation
Granule Release
Dense
Alpha
ADP, 5HT, Ca2+
PF4, βTG, PDGF, vWF Fibrinogen, Fibronectin

aggregation associated with secretion [40]. Moreover, the ability to modulate Ca^{2+} pools are essential to achieve complete activation leading to platelet secretion and clot retraction.

4 (iv) PLATELET ADHESION

Platelet adhesion to subendothelium is the first major step in hemostasis [2,41]. Adhesion is an event mediated by the surface of the platelet and therefore is dependent upon structures found on the plasma membrane. Adhesion involves direct interaction of the platelet membrane with factors made available by endothelial damage or with a foreign surface [42]. Like platelet aggregation, adhesion is initiated by a specific stimulus (e.g., collagen fibers) interacting with a recognition site, (e.g., the collagen receptor). There is specificity in platelet adhesion. Under normal conditions, platelets do not adhere to endothelial cells nor to other blood cells with which they collide in the circulation. Adhesion occurs only with appropriate stimulus such as that following vessel injury and exclusively involves other platelets and the subendothelium.

Since the platelet membrane is rich in glycoproteins, a specific type may interact with the subendothelium. It is also possible that some molecular species acts a bridge between the platelet-subendothelium surfaces. Evidence derived from the study of disease states of adhesion indicates that adhesion depends on both a specific membrane glycoprotein (Glycoprotein Ib (GP Ib)) and a specific plasma protein (von Willebrand factor (vWf)) [43,44]. Reduced adhesion of platelets to subendothelium is observed in von Willebrand's disease, a disorder in which the plasma protein (Factor VIII:vWf complex) is deficient. In Bernard Soulier Syndrome, reduced adhesion occurs as a result of deficient

GP Ib. Evidence also suggests a major role in adhesion for another adhesive protein, fibronectin, which can bind to GP IIb-IIIa [24].

Another platelet glycoprotein, GP Ia, plays an important role in in vivo adhesion by possibly serving as the receptor for collagen [45]. The GP Ia-collagen interaction appears related to platelet spreading whereas GP Ib interaction with vWf allows initial attachment to the subendothelium. Alternatively, GP Ia may interact with another cofactor of platelet adhesion to collagen. Some evidence suggests that this cofactor may be fibronectin [46]. Moreover, GP Ia demonstrates interaction with the platelet cytoskeleton, specifically with actin-binding protein, as well as with GP Ib. Thus, GP Ia and GP Ib may interact indirectly to both mediate and stabilize platelet adhesion.

An experimental technique developed by Baumgartner, which involves perfusion of vascular tissue, is considered an accurate model of in vivo adhesion [47]. However, it has disadvantages with respect to standardization and is difficult to employ routinely. Another in vitro model exists to study platelet adhesion [48]. This model employs ristocetin, an antibiotic effective against gram positive bacteria, as a platelet agglutination agent. Agglutination is a passive surface mediated cross linking of platelets that does not require intraplatelet activation. As such, formaldehyde-fixed platelets can be agglutinated. Ristocetin-induced agglutination is similar to platelet adhesion in that both require the same plasma adhesive protein, namely Factor VIII-vWf, as well as the same platelet membrane component, GP Ib. Studies of Bernard Soulier Syndrome, a platelet disorder characterized by lack of adhesion to subendothelium despite normal amounts of plasma vWf, had indicated the involvement of a specific glycoprotein in agglutination [49]. Ristocetin-induced

agglutination is routinely used as a diagnostic test for von Willebrand's disease, a disorder of platelet adhesion due to plasma vWf deficiency.

The molecular interactions between Factor VIII-vWf, ristocetin and glycoprotein Ib in agglutination are unclear. Studies had suggested that ristocetin either 1) bridges the interaction of Factor VIII-vWf with the membrane surface, or 2) binds to and induces a structural change on Factor VIII-vWf so that the latter can bind platelets [50,51]. More recent observations suggest that ristocetin induces multimer formation of vWf, which in turn cross-links platelets and can mediate platelet adhesion to subendothelium [52]. It is possible that ristocetin-induced agglutination does not involve the same biochemical events as those occurring with physiological activators causing platelet aggregation.

Since agglutination is a passive, surface membrane-mediated cross-linking of cells, it is dependent upon the GP Ib "receptor" properties (i.e., number per unit area, availability or affinity) and the size of the platelets affecting collision frequencies. This would be true assuming that vWf and ristocetin are not limiting factors. Thus, the kinetics of agglutination are influenced by platelet volume fraction ($v \times N_o$), which also reflects the amount of surface area available for passive cross-linkage. Therefore, studies of the kinetics of ristocetin-induced agglutination would require control of the volume fraction parameter, as described in section 7.

4 (v) PLATELET AGGREGATION.

In the hemostatic response, platelets adhere to exposed subendothelium, followed by deposition of more platelets to form an unstable platelet plug. Platelets near the site of injury adhere to an initial platelet layer either as

singlets or in the form of aggregates. Aggregation occurs following the secretion of material from adherent platelets (e.g., ADP) which activates newly arriving single platelets. The latter change shape and upon collision with other platelets, adhere to each other and/or the initial platelet layer. Aggregation of platelets is a specialized form of adhesion, involving some common and distinct biochemical requirements from that of adhesion to sub-endothelium.

Platelet aggregation has been subdivided into two sequential categories [53]. Figure 6 depicts a simple scheme of platelet aggregation showing a two stage process. Platelet microaggregation (PA) refers to formation of early aggregates consisting of <10 platelets per aggregate, derived from the recruitment of single platelets. Under appropriate conditions, such as flow at low shear rates, macroaggregation (TA) can occur with weak to moderate activation of platelets, i.e., the formation of much larger, visible aggregates (>> 10 platelets per aggregate) from the build-up of the smaller micro-aggregates. Because these macro-aggregates are mechanically unstable, slight increases in shear rate induce reversion to micro-aggregates. However, with stronger activation induced, typically, by high agonist concentrations (e.g., 2 to 3 μM ADP), secondary stable aggregation is attained with accompanying platelet secretion even at high flow rates.

Evidence suggests that the two processes of aggregation (PA and TA), have distinct time and agonist concentration dependencies [39,53]. Typically, single platelets are maximally recruited into doublets, triplets and higher multiplets by ~10 seconds post activation at which time TA has achieved < 10% of its maximum response. Sensitivity as expressed by activator concentrations required to induce half maximal rates of aggregation, e.g., $[ADP]_{1/2}$, is much lower for PA than for TA. In addition, they are distinct with respect to sensitivity to inhibitors and

Figure 6. The sequence of platelet activation leading to irreversible macro-aggregation. It consists of 3 main processes having distinct activation requirements: shape change (SC), micro-aggregation (PA), and macro-aggregation (TA). Fn-Ca refers to the co-factors required for both PA and TA. Figure shown on next page.

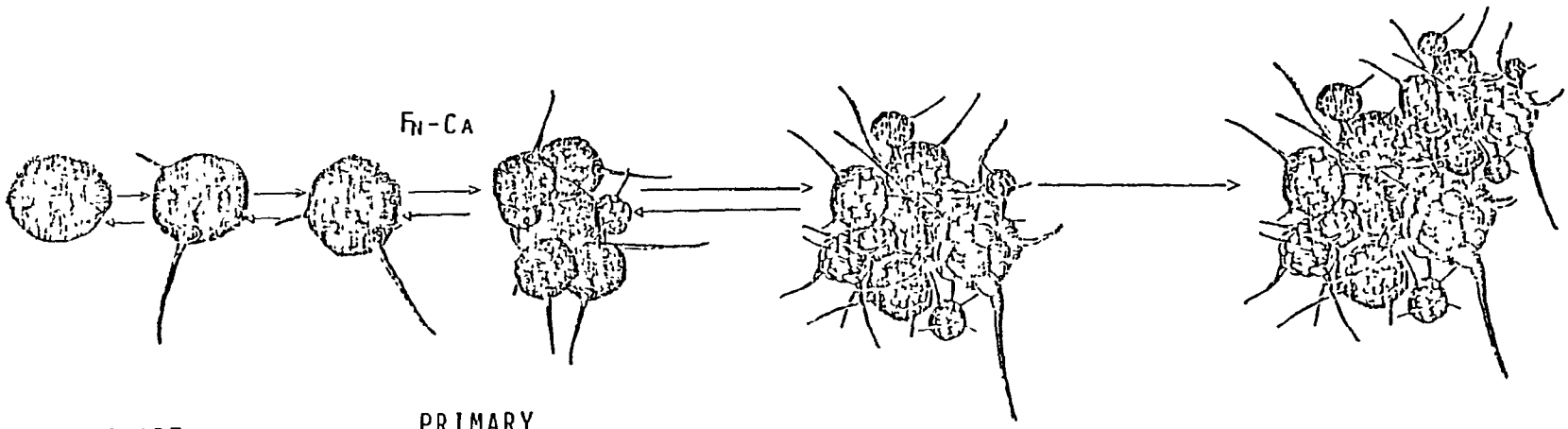

SHAPE CHANGE

PRIMARY AGGREGATION PA

REVERSIBLE MACROAGGREGATION TA-1

STABLE MACROAGGREGATION TA-2

refractoriness. Platelet refractoriness, or loss of sensitivity to agonist, may occur in the interval between micro-aggregate to macro-aggregate formation, but not during micro-aggregate formation from single platelets [53].

The most common method of in vitro study of platelet aggregation involves the monitoring of visible light transmittance through a stirred suspension of platelet-rich plasma (aggregometry). Changes in plasma turbidity are recorded following addition of activators. Typical tracings obtained for many types of agonist induced responses consist of distinct phases that represent platelet shape change and macroaggregation.

The initial decrease in %T in the first 4-5 seconds following activator addition reflects platelet shape change to disco-echinocyte forms [5]. Under optimal stimulus, aggregation occurs biphasically and is so represented in aggregometry tracings by a two phase increase in light transmission (Figure 7). Primary aggregation (TA-1) refers to the initial portion of %T rise associated with the aggregation of all platelets present. This initial aggregation will revert in the absence of platelet secretion. Secondary aggregation (TA-2) occurs with platelet secretion and is associated with the build-up of even larger aggregates than those obtained in TA-1, with each aggregate becoming more compact [53].

The study of aggregation in terms of micro- and macro-aggregation, requires two distinct methodologies. Whereas conventional light transmission aggregometry can monitor TA, it is insensitive to the detection of microaggregation. This is because most platelets (> 80%) will form micro-aggregates containing up to 7 platelets per aggregate before any increase in %T is detected. Particle measurements done by microscopy or electronic counting are required to study PA. Microaggregation can be measured from the decrease in the number of non-aggregated or single platelets. The time

Figure 7. Representative example of an aggregometry tracing showing agonist (A)-induced platelet shape change and bi-phasic aggregation (TA-1 & TA-2) in platelet-rich plasma (c-PRP). Changes in % light transmission are recorded continuously as a function of time. Kinetic parameters of aggregation shown are: rate of shape change (V_S), rate of macroaggregation (V_a), and maximal extent of aggregation (%Tmax). (Modified from Tang S S and Frojmovic M M. J Lab Clin Med 1980:95;243)

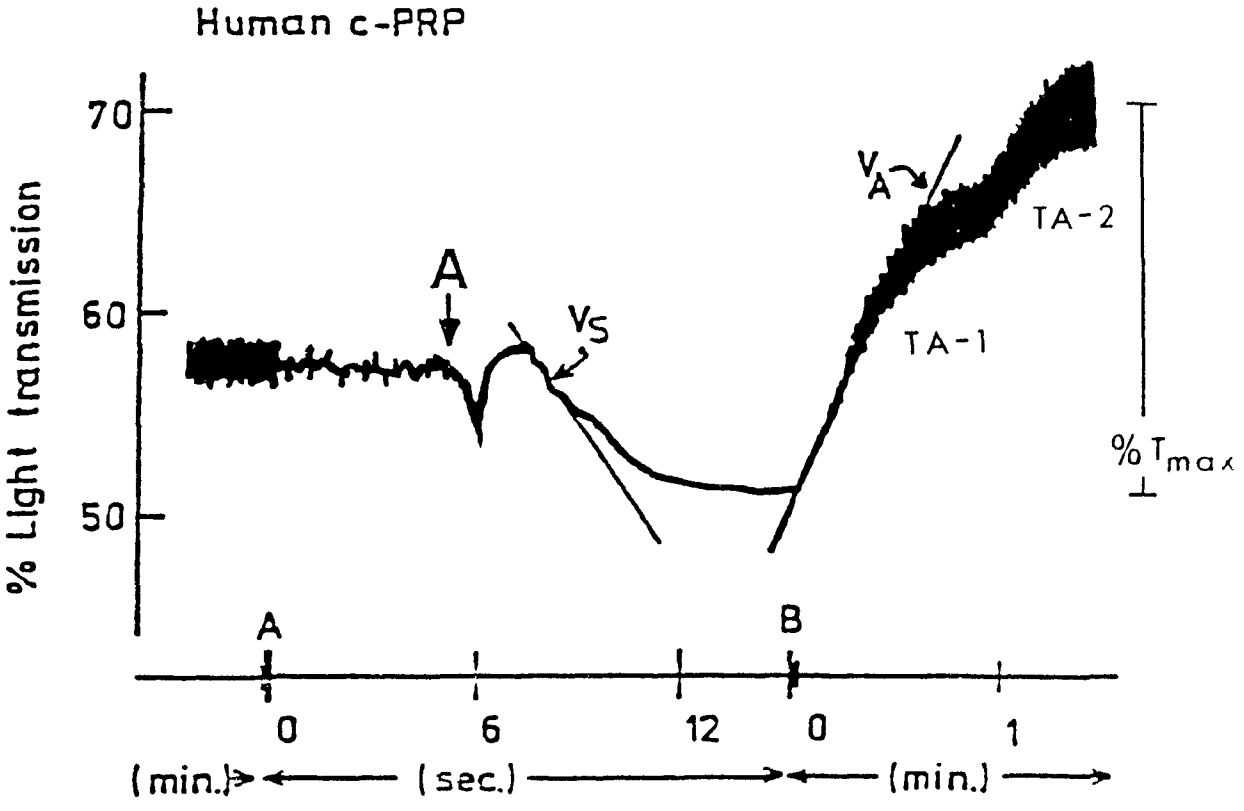

course for PA following the addition of various concentrations of ADP to stirred platelet rich plasma is shown in Figure 8 [53]. The onset of shape change involving pseudopod extrusion precedes microaggregation, underscoring the importance of echinocyte formation. This lag time of about 1 second corresponds to an activation step independent of external calcium. The PA response with time appears S-shaped, with an initial rapid linear increase between 1 and 4 seconds, during which time doublet and triplet formation occurs. PA attains a maximum by ~10 seconds, corresponding to the maximal disappearance of single platelets into micro-aggregates [53].

Aside from experimental differences, the concept of two distinct processes of aggregation is supported by observations that fibrinogen binds to activated platelets with distinct affinities [54,55]. Differential aggregation responses for PA and TA would be characterized by distinct expression of numbers and/or affinities of GP IIb-IIIa on activated platelets. Thus, PA might require fewer FBS expressed with highest affinity for Fn, with low activation conditions, while TA would require more FBS per platelet to provide stronger Fn-mediated platelet cross-linking to resist shear(flow)- induced disaggregation. Finally, different responses to the same stimulus by sub-populations of platelets) could be attributable to differences with respect to FBS characteristics as well as to other biochemical differences between platelet sub-populations (see Section 6).

Figure 8. Time courses of ADP-induced microaggregation (PA) at various activator concentrations. Percent PA was determined as a function of time after ADP addition to stirred platelet-rich plasma, and assessed by microscopy from the decrease in single platelets. The initial linear rate of PA can be readily determined, typically represented by PA at t=3 seconds. (From: Frojmovic M M, et al. J Lab Clin Med 1983:101;96)

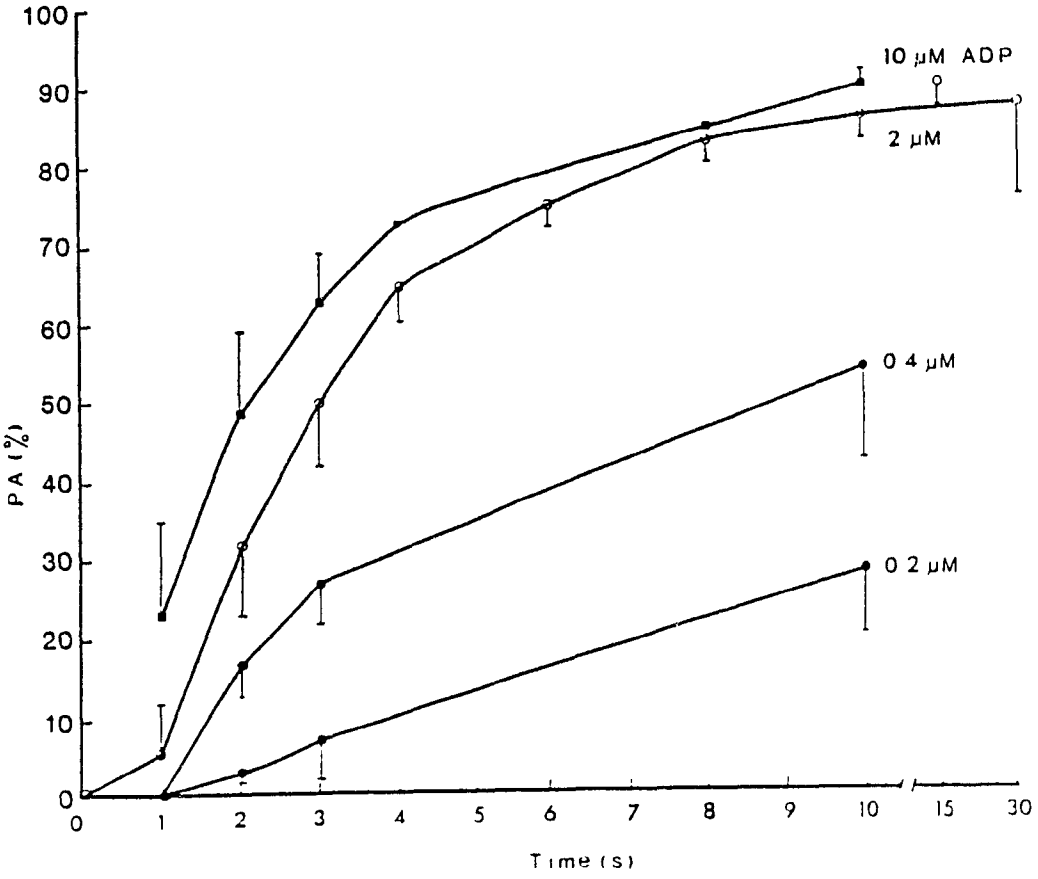

5. PLATELET PRODUCTION

Platelets are derived from the fragmentation of bone marrow megakaryocytes (MK) [56,57]. The latter is a specialized cell of an exclusively committed stem cell line, which in turn derives from a precursor pluripotent cell common to both myeloid and erythroid cells (Figure 9). Megakaryocytes are nucleated cells which synthesize platelet proteins, assemble platelet organelles and give rise to platelets only upon reaching full maturation. Platelet production is under the control of a humoral factor, thrombopoietin, which stimulates the proliferation of committed stem cells.

The time interval between the transformation of a stem cell into a platelet-producing MK is about 10 days, comparable to the average life span of a platelet. Once the committed stem cell becomes a megakaryocyte, it undergoes a unique stage of maturation distinct from common binary cell division. The growing MK enters endomitosis whereby it matures without cellular division. Thus maturing MK's become larger and can be sub-classified according to "ploidy", i.e., the number of nuclear doublings (N) undergone. There is a correlation between the size of a MK and its respective number of nucleii [56]. The three principal classes of MK which eventually give rise to platelets are the 8N, 16N and 32N ploidy classes. Each respective ploidy class matures to produce platelets, with the greatest contribution made by the 16N class. Megakaryocytes produce and accumulate platelet specific materials (e.g., platelet factor 4, ß-thromboglobulin) during maturation [58].

During maturation, the MK cytoplasm develops a large network of demarcation membranes which are actually extensions of the MK plasma membrane [59]. Observations have shown the demarcation membranes to be in the form of tubules and flattened cysternae that undergo branching. The

membranes appear to arise from the plasma membrane by invagination. It is thought that the demarcation membrane system delineates platelets within the cytoplasm of megakaryocytes.

Simultaneous with cytoplasmic maturation, the nucleus undergoes changes in appearance that correlate with nuclear division. Initially, the early stage MK nucleus is multi-lobed and contains relatively little cytoplasm. With further maturation, the nuclear material becomes more compact while the cytoplasm, i.e., demarcation membranes, become larger.

The formation of platelet precursors involves extension of the MK cytoplasm into the sinusoids of the bone marrow [60]. This is then followed by the pinching off of these processes to give rise to pro-platelets [61]. These pre-cursor fragments often contain more than one potential platelet. Platelets therefore are not produced by direct shedding from megakaryocyte cytoplasm within the bone marrow. Some evidence suggests that between 20 to 50% of mature MKs are released into the circulation as intact cells [57,61].

Large fragments broken off from megakaryocyte processes undergo further fragmentation as well as internal re-organization to yield platelets. Division of the pro platelets into bona fide platelets occurs readily in the lung microvasculature [62]. Large fragments, or MKs would be trapped in the pulmonary microvasculature. It has been suggested that the regular movements associated with breathing may provide the mechanical force required to cause further breakage into individual platelets. Megakaryocytes at maturity can each give rise to about 1000 - 3000 platelets. With normal platelet turnover in man at about 8-9 billion per hour, the corresponding MK turnover would be about 4 - 5 million per hour [63].

Figure 9. A: A model showing similarities in the production of three major blood cell types originating from common pluripotent stem cells. Each cell line likely has its own subsequent committed stem cells and regulator(s)(-Poietins(s)) of production.
B: A model of megakaryocyte (MK) maturation and platelet production. Growth of MK's is characterized by nuclear enlargement due to endoreplication and the yielding of polyploidy MK's (e.g., 16N). MK cytoplasmic development precedes fragmentation into pro-platelets. (From: Ebbe S. Biology of Megakaryocytes. In: Prog Hemost Thrombos, Vol.3, Grune and Stratton, New York 1976.)

A.

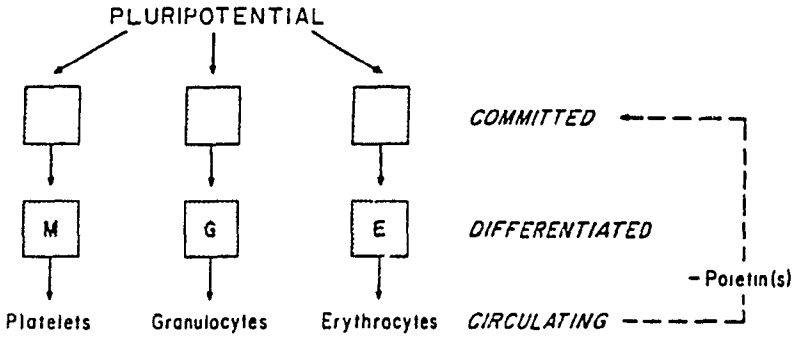

B.

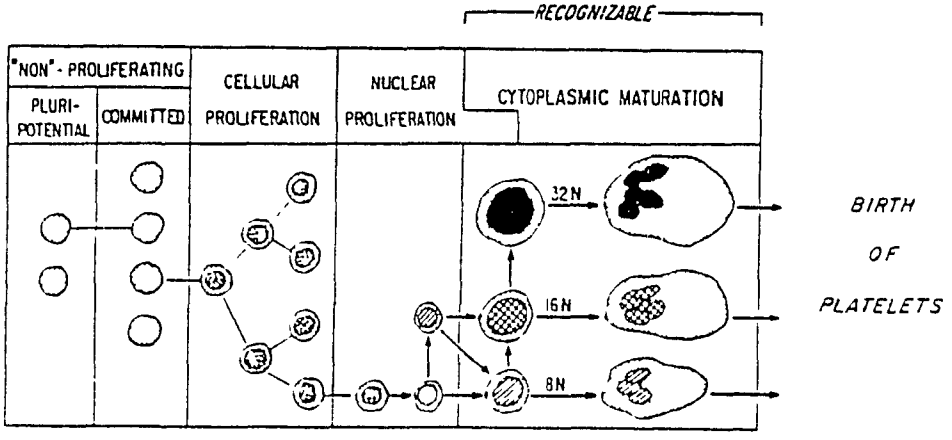

6. PLATELET HETEROGENEITY

Much evidence suggests that circulating platelets are heterogeneous with respect to density, volume, ultrastructure, biochemical content and related function [56, 64-66]. Figure 10 illustrates the heterogeneity and inter-relationships between megakaryocytes and platelets and their cellular properties. The basis of platelet heterogeneity is unresolved, i.e., whether platelet diversity arises from production characteristics or as a consequence of aging or both. For example, some investigators have suggested that platelet aging in circulation is associated with a simultaneous decrease in platelet density [64,67]. Platelet heterogeneity would be a consequence of senescence in the circulation whereby large, heavy platelets become small, lighter ones with age. Others have reported an increase in density with age or that density heterogeneity is determined during megakaryocyte maturation [56]. In the latter case, platelets of a particular density would originate from megakaryocytes of a particular ploidy class.

These apparent contradictory findings may have arisen from differences in methods of platelet isolation, but opposite conclusions have been drawn by investigators employing the same technique. Methods using differential centrifugation [68], density and functional separation have yielded conflicting results for functional measurements and associated platelet size, age, density and metabolism.

The unique process of megakaryocyte maturation and subsequent platelet production is thought to give rise to heterogeneous platelets [56]. The three major ploidy classes are the 8N, 16N and 32N. Megakaryocytes from these ploidy classes have been shown to differ with respect to cytoplasmic properties, and therefore platelets arising from each class would expect to carry over these differences. The

Figure 10. Table showing trends of platelet characteristics as a function of MK ploidy. Arrows indicate increasing (↑) or decreasing (↓) trends with the associated MK ploidy . Data is derived from studies in several mammalian species.

Megakaryocyte Ploidy	PLATELET				
	Size	Density	Mitochondria + Granules #/fl	Internal Membranes Incl. SCCS	DTS + Activity
8 n (small(s))	↑(L)	↑	↑	↓	↓
16 n (medium)			average values		
32 n (large (L)	↓(S)	↓	↓	↑	↑

differences between the three types of megakaryocytes would constitute a source of heterogeneity. This appears to be true in light of findings in these studies that 8N megakaryocytes give rise to denser and larger platelets which have greater content of granules and organelles per unit volume than smaller, less dense ones [56]. The denser, larger platelets also appear to have less invaginated SCCS membrane. These density and size-dependent differences may have functional significance.

Earlier studies which isolated platelets on the basis of differing density had established that circulating platelets are heterogeneous with respect to physical properties and function [65,69]. The investigators had ascribed these density related differences to aging. Subsequent studies however showed that platelets of varying density are released simultaneously; therefore differences would be present regardless of aging [70].

Platelet size appears to be a determinant of platelet function. Platelet aggregation assessed in whole platelet populations as measured from aggregometry showed that aggregation velocity was proportional to platelet volume [67]. The response correlated best with the megathrombocyte index which indicates the relative number of large sized platelets present.

There are methods for actual physical isolation of size-dependent fractions from whole platelet populations. Counterflow centrifugation takes advantage of the > 200% difference in size of large versus small platelets compared to < 5% differences in density, and separates platelets into different size fractions having relatively less overlap between fractions than other methods. Investigators using this method found platelet size to be a determinant of function and biochemical properties [66,71]. Platelet function as measured by aggregation, release and serotonin uptake was found to be faster and/or more extensive for the

largest sized platelets.

Further experiments by this group showed significant positive correlations between platelet volume and rates and extents of aggregation as measured by aggregometry [71]. However, these studies were conducted for different-sized platelets at identical platelet counts thereby ignoring contributions of total platelet mass to observed rates of aggregation. Size-dependent responses were seen for ADP- and thrombin- induced aggregation, but not for ristocetin-induced agglutination. Other biochemical properties such as ATP content were also shown to be size dependent. These investigators concluded that the intrinsic function of platelets was similar but their absolute capacities correlate with size. Subsequently, it was shown that platelet size and age are both determinants of function that act independently [72]. In these studies, platelet size was found to be a geometric determinant of aggregation rates. However, the relationship between platelet membrane mass versus intrinsic membrane biochemical differences could not be quantitatively interpreted because aggregation was assessed at identical platelet counts for the different sized fractions.

Measures of aggregation kinetics and sensitivity by particle counting methods have also been reported for platelets separated by functional and differential centrifugation [68,73]. In functional fractionation, the reactive platelets were separated from the less reactive ones by exposure of whole platelet populations to low doses of activator. This induced aggregation of the reactive platelets, which were isolated by light centrifugation, followed by their disaggregation into single platelets. These highly reactive platelets were not refractory to further activation and were thus re-challenged with activator, as were the less reactive ones. Whole platelet populations were separated into size- and density- dependent

fractions following differential centrifugation by removal of the top PRP layer following its centrifugation at various g forces. However, both of these methods yield platelet fractions with large overlap in similar sized platelets. Larger-sized platelets aggregated with greater sensitivity but with less rapidity. Larger platelets contained more glycogen and surface sialic acid; even when normalized for volume. Aging patterns also appeared to be distinct for these functionally separated fractions.

7. CONTRIBUTION OF PLATELET MASS TO PLATELET AGGREGATION.

Studies of platelet aggregation on subpopulations separated on the basis of either size or density have generally supported the idea that young platelets which are large and dense are the most functionally active. Aggregation studies to-date have not focussed on the contributions of platelet mean volume (v), platelet number (N_o) and the product of these two, i.e., the volume fraction ($\emptyset$) to aggregation responses. From a kinetic point of view, these are determinants of platelet aggregation which must be accounted for in establishing platelet aggregability. For platelets considered as particles, the rate of aggregation in simple shear flow is generally expressed as the decrease in particle count ($-dN_t/dt$) where,

$$\text{Platelet aggregation} = \frac{dN_t}{dt} = \frac{-4G\emptyset}{\pi} Nt \times \alpha_G \qquad (1)$$

where $\emptyset$ is the volume fraction (v x N_t) of the particles, G is the rate of shear, N_t is the particle concentration at time t following platelet activation, and α_G is the particle collision efficiency [74]. This equation is

expected to describe the rate of microaggregation (PA) and may carry over to a description of TA. It is clear from equation (1) that aggregation kinetics will be influenced by the platelet volume fraction ($v \times N_t$). In order to know, or to have a comparative idea of how α behaves, it is necessary to control platelet volume fraction and/or flow conditions. By directly relating aggregation and α, one can get an idea of the collision efficiency which indicates the intrinsic ability of platelets to aggregate. The α value reflects the efficiency of generation of platelet membrane stickiness, which in turn depends on the dynamics of expression of fibrinogen binding sites on activated platelets. Thus, comparative studies of platelet aggregation kinetics between different-sized populations would require control of variables which affect the collision frequency (G, $\emptyset$) in order to compare α. This is readily done by comparing distinctly-sized platelet suspensions under identical flow (stir) conditions and at comparable volume fractions. Experimentally, distinctly sized-fractions can be obtained by counter-flow centrifugation [71,75] and be compared for aggregation responses at controlled volume fractions.

REFERENCES

1) Frojmovic M M, Milton J G. Platelet size and shape in health and disease. Physiol Rev 1982;62:185-261.

2) Gordon J L. Platelets in perspective. In: Platelets in biology and pathology, Vol.2. Gordon J L (ed.),pp 1-17. Elsevier/North-Holland, Amsterdam 1981.

3) Zucker M B. Platelet function. In: Hematology. Williams W J (ed.),pp 1200-1209. McGraw-Hill, New York 1977.

4) Sinzinger H. Role of platelets in atherosclerosis. Sem Thromb Hemost 1986;12;124-133.

5) Frojmovic M M, Milton J G. Physical, chemical and functional changes following platelet activation in normal and "giant" platelets. Blood Cells 1983;9:359-382.

6) Holmsen H. Platelet secretion. In: Hemostasis and Thrombosis. Colman R W, Hirsh J, Marder V J, Salzman E W (eds.),pp 390-403. J B Lippincott Co., Toronto 1982.

7) White J G. Ultrastructural physiology and cytochemistry of blood platelets. In: The Platelet. Brinkhous K M, Mostafi F K (eds.),pp 83-115. Williams and Wilkins, Baltimore 1971.

8) White J G, Gerrard J M. Anatomy and structural organization of the platelet. In : Hemostasis and Thrombosis. Colman R W, Hirsch J, Marder V J, Salzman E W (eds.),pp 343-363. J B Lippincott Co., Toronto 1982.

9) White J G. Interaction of membrane systems in blood platelets. Am J Path 1972;66:295-312.

10) Phillips D R. Platelet membranes and receptor function. In: Hemostasis and Thrombosis. Colman R W, Hirsch J, Marder V J, Salzman E W (eds.),pp 444-458. J B Lippincott Co., Toronto 1982.

11) Nurden A T, George J N, Philips D R. Platelet membrane glycoproteins: their structure, function, and modification in disease. In: Biochemistry of Platelets. Phillips D R, Shuman M A.(eds.),pp 159-224. Academic Press, New York 1986.

12) Barber A J, Jamieson G A. Isolation and characterization of human blood platelet membranes. J Biol Chem 1970;245:6357-6365.

13) Philips D R, Charo I F, Parise L V, Fitzgerald L A. The platelet membrane glycoprotein IIb-IIIa complex. Blood 1988:71;831-843.

14) Pytela R, Pierschbacher M D, Ginsberg M, Plow E F, Ruoslahti E. Platelet membrane glycoprotein IIb/IIIa: member of a family of Arg-Gly-Asp-specific adhesion receptors. Science 1986:231;1559-1562.

15) Sixma J J. Platelet Adhesion in health and disease. In: Thrombosis and Haemostasis 1987. Verstraete M, Vermylen J, Lijnen R, Arnout J (eds.),pp 127-146. Leuven University Press, Leuven (Belgium) 1987.

16) Phillips D R. Effect of trypsin on the exposed polypepetides and glycoproteins in the human platelet membrane. Biochem 1972;11;4582-4588.

17) O'Farrell P H. High resolution two-dimensional electrophoresis of proteins. J Biol Chem 1975;250:4007-4021.

18) Philips D R, Agin P P. Platelet plasma membrane glycoproteins. Evidence for the presence of nonequivalent disulfide bonds using nonreduced-reduced two-dimensional gel electrophoresis. J Biol Chem 1977;252:2121-2126.

19) Shattil S J, Hoxie J A, Cunningham M, Brass L F. Changes in the platelet membrane glycoprotein IIb-IIIa complex during platelet activation. J Biol Chem 1985:260;11107-11114.

20) Asch A S, Leung L L K, Polley M J, Nachman R L. Platelet membrane topography:colocalization of thrombospondin and fibrinogen with the glycoprotein IIb-IIIa complex. Blood 1985;66:926-934.

21) Tuszynski G P, Rothman V L, Murphy A, Siegler K, Knudsen K A. Thrombospondin promotes platelet aggregation. Blood 1988:72;109-115.

22) Nurden A T. Platelet membrane glycoproteins and their clinical aspects. In:Thrombosis and Haemostasis 1987. Verstraete M, Vermylen J, Lijnen R, Arnout J (eds.),pp 93-125. Leuven University Press, Leuven (Belgium) 1987.

23) Parise L V, Phillips D R. Fibronectin-binding properties of the purified platelet glycoprotein IIb-IIa complex. J Biol Chem 1986;261:14011-14017.

24) Plow EF, McEver R P, Coller B S, Woods V L, Marguerie G A, Ginsberg M H. Related binding mechanisms for fibrinogen, fibronectin, von Willebrand factor, and thrombospondin on thrombin-stimulated human platelets. Blood 1985:66;724-727.

25) Nachman R L, Leung L L K. Complex formation of platelet membrane glycooroteins IIb-IIIa with fibrinogen. J Clin Invest 1982;69;263-269.

26) Gear A R L. Preaggregation reactions of platelets. Blood 1981:58;477-490.

27) Milton J G, Frojmovic M M. Turbidometric evaluations of platelet activation: relative contributions of measured shape change, volume, and early aggregation. J Pharmacol Methods 1983:9;101-115.

28) Frojmovic M M. Rheooptical studies of platelet structure and function. In: Progress in Hemostasis and Thrombosis. Vol 4. Spaet T H (ed.), pp 279-320, Grune and Stratton, New York 1978.

29) Milton J G, Frojmovic M M. Adrenaline and adenosine diphosphate-induced platelet aggregation require shape change. J Lab Clin Med 1984:104;805-815.

30) Tang S S, Frojmovic M M. Inhibition of platelet function by antithrombotic agents which selectively inhibit low-K_m cyclic 3',5'-adenosine monophosphate phosphodiesterase. J Lab Clin Med 1980:95;241-257.

31) Cohen I. Contractile platelet proteins. In: Hemostasis and Thrombosis. Colman R W, Hirsh J, Marder V J, Salzman E W.(eds.),pp 459-471. J B Lippincott, Toronto 1982.

32) Weiss L. Cellular locomotive pressure in relation to initial cell contacts. J Theor Biol 1964:6;275-281.

33) Marsh S A, Jones G E. Microspike function in cell aggregation. Eur J Cell Biol 1982:28;278-280.

34) Ware J A, Johnson P C, Smith M, Salzman E W. Effect of common agonists on cytoplasmic ionized calcium concentration in platelets. J Clin Invest 1986:77;878-886.

35) Hallam T J, Sanchez A, Rink T J. Stimulus-response coupling in human platelets. Biochem J 1984:218;819-827.

36) Kishimoto A, Takai Y, Mori T, Kikkawa U, Nishizuka Y. Activation of calcium and phospholipid-dependent protein kinase by diacylglycerol, its possible relation to phosphatidylinositol turnover. J Biol Chem 1980:255;2273-2276.

37) Berridge M J, Irvine R F. Inositol triphosphate, a novel second messenger in cellular signal transduction. Nature 1984:312;315-321.

38) Haslam R J. Signal transduction in platelet activation. In: Thrombosis and Haemostasis. Verstraete M, Vermylen J, Lijnen R, Arnout J. (eds.), pp 147-174. Leuven University Press, Leuven 1987.

39) Pedvis L G, Wong T, Frojmovic M M. Differential Inhibition of the platelet activation sequence: shape change, micro- and macro-aggregation, by a stable prostacyclin analogue (Iloprost). Thrombos Haemost 1988:59;323-328.

40) Rink R J, Smith S W, Tsien R Y. Cytoplasmic free Ca2+ in human platelets: Ca2+ thresholds and Ca-independent activation for shape-changed and secretion. FEBS Letter 1982:148;21-27.

41) Packham M A, Mustard J F. Platelet Adhesion. In: Progress in Hemostasis and Thrombosis. Spaet T H (Ed.), pp 211-288. Grune and Stratton, Orlando 1984.

42) Mohamad S F, Hardison M D, Clenn C H, Morton B D, Bolan J C, Mason R G. Adhesion of human blood platelets to glass and polymer surfaces. Haemostasis 1974;3:257-270.

43) Hardisty R M. Disorders of platelet function. Br Med Bull 1977;33;207-212.

44) Girma J P, Meyer D, Verweij L, Pannekoek H, Sixma J J. Structure-function relationship of human von Willebrand factor. Blood 1987;70:605-612.

45) Niewenhuis H K, Sakariassen K S, Houdijk W P M, Nievelstein P, Sixma J J. Deficiency pf platelet membrane glycoprotein Ia associated with a decreased platelet adhesion to subendothelium: a defect in platelet spreading. Blood 1986:68;692-695.

46) Houdijk W P M, Sakariassen K S, Nievelstein P, Sixma J J. Role of factor VIII-von Willebrand factor and fibronectin in the interaction of platelets in flowing blood with monomeric and fibrillar collagen types I and II. J Clin Invest 1985:75;531-540.

47) Baumgartner H R. The role of blood flow in platelet adhesion, fibrin deposition and formation of mural thrombi. Microvasc Res 1973:5;167-179.

48) Howard M A, Firkin B G. Ristocetin: a new tool in the investigation of platelet aggregation. Thromb Diath Haemorrh 1971;26;362-369.

49) Bernard J, Soulier J-P. Sur une nouvelle variété de dystrophie thrombocytaire-hémorragitaire congénitale. Sem Hop Paris 1948:24;3217-3223.

50) Jenkins C S P, Meyer D, Dreyfus M D. Willebrand factor and ristocetin. I. Mechanism of ristocetin-induced platelet aggregation. Br J Haematol 1974:28;561-578.

51) Kao K J, Pizzo S V, McKee P A. Demonstration and characterization of specific binding sites for factor VIII/von Willebrand factor on human platelets. J Clin Invest 1979:63;656-664.

52) Jenkins C S P, Clemetson K J, Luscher E F. Studies on the mechanism of ristocetin-induced platelet agglutination: binding of ristocetin to platelets. J Lab Clin Med 1979:93;220-231.

53) Frojmovic M M, Milton J G, Duchastel A. Microscopic measurements of platelet aggregation reveal a low ADP -dependent process distinct from turbidometrically measured aggregation. J Lab Clin Med 1983:101;964-976.

54) Peerschke E I B. Evidence for interaction between platelet fibrinogen receptors. Blood 1982:60;973-978.

55) Niewiarowski S, Kornecki E, Budzynski A Z, Morenelli T A, Tuszynski G P. Fibrinogen interaction with platelet receptors. Ann NY Acad Sci 1983:408;536-555.

56) Penington D G, Streatfield K, Roxburgh A E. Megakaryocytes and the heterogeneity of circulating platelets. B J Haematol 1976:34;639-653.

57) Levin J. Thrombopoiesis. In: Hemostasis and Thrombosis. Colman R W, Hirsh J, Marder V J, Salzman E W. (eds.), pp 225-236. J B Lippincott, Toronto 1982.

58) Penington D G. Formation of Platelets. In:Platelets in biology and pathology-2. Dingle J T, Gordon J L. (eds.),pp 19-41. Elsevier/North Holland Biomedical, Amsterdam 1981.

59) Behnke O, Pedersen N T. Ultrastructural aspects of megakaryocyte maturation and platelet release. In: Platelets. Production, Function, Transfusion and Storage. Baldini M G, Ebbe S (eds.),pp 21-31. Grune and Stratton, New York 1974.

60) Thiery J B, Bessis M. La genèse des plaquettes à partir des mégacaryocytes observés sur la cellule vivante. C R Acad Sci 1956:242;290-297.

61) Tong S, Seth P, Penington D G. Proplatelets and stress platelets. Blood 1987:69;522-528.

62) Trowbridge E A, Martin J F, Slater D N. Evidence for a theory of physical fragmentation of megakaryocytes, implying that all platelets are produced in the pulmonary circulation. Thromb Res 1982:28;461-475.

63) Hanson S R, Slichter S J. Platelet kinetics in patients with bone marrow hypoplasia: evidence for a fixed platelet requirement. Blood 1985:66;1105-1109.

64) Karpatkin S. Heterogeneity of human platelets. II. Functional evidence suggestive of young and old platelets. J Clin Invest 1969:48;1083-1087.

65) Corash L, Costa J L, Shafer B, Donlon J A, Murphy D. Heterogeneity of human whole blood subpopulations. III. Density-dependent differences in subcellular constituents. Blood 1984:64;185-193.

66) Thompson C B, Eaton K A, Princiotta S M, Rushin C A. Valeri C R. Size dependent platelet subpopulation relationships of platelet volume to ultrastructure enzymatic activity and function. Brit J Haematol 1982:50;509-519.

67) Karpatkin S. Heterogeneity of human platelets. VI. Correlation of platelet function with platelet volume. Blood 1978:51;307-316.

68) Carty D J, Gear A R L. Fractionation of platelets according to size: functional and biochemical characteristics. Am J Haem 1986:21;1-6.

69) Leone G, Agostini A, DeCrescenzo A, Bizzi B. Platelet heterogeneity: relationship between buoyant density, size, lipid peroxidation and platelet age. Scand J Haem 1979:23;204-210.

70) Ebbe S. Biology of megakaryocytes. In: Progress in hemostasis and thrombosis. Vol. 3. Spaet T (ed.), pp 211-229. Grune and Stratton, New York 1976.

71) Thompson C B, Jakubowski J A, Quinn P G, Deykin D, Valeri C R. Platelet size as a determinant of platelet function. J Lab Clin Med 1983:101;205-213.

72) Thompson C B, Jakubowski J A, Quinn P G, Deykin D, Valeri C R. Platelet size and age determine platelet function independently. Blood 1984:63;1372-1375.

73) Haver V M, Gear A R L. Functional fractionation of platelets. J Lab Clin Med 1981:97;187-204.

74) Chang H N, Robertson C R. Platelet aggregation by laminar shear and Brownian motion. Ann Biomed Eng 1976:4;151-183.

75) Lindahl P E. Principle of a counter-streaming centrifuge for the separation of particles of different sizes. Nature 1948:16;648-649.

CHAPTER II

PLATELET SIZE-DEPENDENT SUBPOPULATIONS: RELATIVE CONTRIBUTIONS OF PLATELET NUMBER, VOLUME FRACTION AND BIOCHEMICAL DIFFERENCES TO MICRO- AND MACRO- AGGREGATION FOR THREE PHYSIOLOGICAL ACTIVATORS AND FOR RISTOCETIN

SUMMARY

The relationship between platelet size (v), platelet number (N_o) and platelet aggregation was evaluated in human platelet subpopulations separated on the basis of volume using counterflow centrifugation. The original platelet population and three size-dependent platelet fractions were concentrated and resuspended in autologous citrated platelet-poor plasma at varying N_o. Microaggregation (PA) and macroaggregation (TA) were determined respectively by electronic particle counting and light transmission (aggregometry). At similar N_o (180±50 x 10^3/ µl), large platelets (L; v = 7.3±0.2 fl; 16±4% of the total population) were about two-fold more sensitive and more rapidly recruited into both micro (PA) and macro (TA) aggregates in response to ADP than the smallest platelets (S; v = 4.2±0.2 fl; 16±3%). At similar volume fraction, however, all the above differences persisted for PA but not for TA; in addition, maximal rates of shape change to ADP were the same for L and S platelets. Although similar results were obtained for two other receptor-mediated platelet activators, namely a stable thromboxane A_2 analogue (U46619) and platelet activating factor (PAF), no significant differences in L vs. S were seen for ristocetin-induced agglutination. The functional differences with receptor-mediated platelet activation appear to arise from intrinsic biochemical differences present in size-dependent subpopulations for which a likely model is proposed.

INTRODUCTION

There is a large body of knowledge describing diverse structural and functional heterogeneity of platelets [1-15], but the precise nature and significance of these differences are still controversial. Methods using density [1,3-8,15], differential centrifugation [8,11], and functional [2] separation have been used yielding conflicting results for functional measurements and associated platelet size, age, density and metabolism [1,3,7-9,13,15]. It does appear that megakaryocytes (MK) of low ploidy yield the largest platelets enriched in organelles and membranes when compared to smaller platelets produced by MK's of high ploidy [6]. Large platelets generally appear metabolically most active [2,9], most responsive to aggregating agents [2,5,10], contain highest concentrations of dense and α-granules [1,6], and appear most efficient in hemostatic effectiveness [5,12-17].

An attempt to relate platelet size to structure and function has recently been made by the elegant use of counterflow centrifugation which takes advantage of the > 200% difference in platelet size between large and small platelets compared to the < 5% differences in density [9]. Previous studies have all generally measured %T changes for different-sized fractions at the same initial platelet counts (N_o) [9,10]. In these studies, platelet size was found to be a geometric determinant of rates of platelet aggregation. However, actual platelet volume fraction vs. intrinsic membrane biochemical differences could not be quantitatively interpreted because turbidometric measurements for the different sized fractions were made at identical N_o. In fact, interpretation of the data in terms of effects of volume fraction versus intrinsic differences in platelet reactivity to form large aggregates is

complicated by recent reports of the physical dependence of turbidimetrically-measured aggregation on platelet number and refractive index; this study suggested that different-sized platelets are better compared for TA studies with initial platelet count (N_o) adjusted to give comparable initial %T ($\%T_o$) values of the platelet suspensions [18].

More specific measures of aggregation kinetics and sensitivity conducted by platelet particle counting methods have been reported for platelets separated functionally and by differential centrifugation but major size overlap existed between the different fractions in these studies. Moreover, the different fractions were studied at the same initial platelet counts [2,11,17]. Here we obtain size-dependent platelet fractions using counterflow-centrifugation and examine their kinetics and sensitivity of aggregation at varying platelet counts induced by physiological activators: adenosine diphosphate (ADP), a stable prostaglandin H_2 analogue (U46619) and platelet activating factor (PAF). We compare platelet macro-aggregation (TA) with particle counting-derived micro-aggregation (PA) since these have previously been shown to have distinct physiological and pharmacological properties for evaluations of unfractionated platelet suspensions [19-21]. We also evaluate the initial rate of ristocetin-induced agglutination, using particle counting. Ristocetin can cause agglutination independent of platelet metabolism and has been reported to cause similar agglutination for different sized fractions evaluated turbidometrically [10]. We found that the greater aggregability of large platelets over small platelets seen with turbidometrically-measured macro-aggregation of platelet suspensions at identical N_o essentially disappears when N_o are adjusted to yield identical initial %T. In addition, with platelet mass adjusted for different-sized fractions, the intermediate to large platelets are most responsive to physiological

activators in terms of both kinetics and sensitivity of micro-aggregation, while no significant differences are observed for ristocetin-induced agglutination. A simple molecular model is proposed to account for the differences.

MATERIALS AND METHODS.

BLOOD COLLECTION AND PLATELET ISOLATION.

Blood was obtained from healthy human donors between the ages of 22 and 34 years. Donors were not on any medication and informed consent was obtained with a protocol approved by a Human Experimentation Committee. Whole blood (WB) was drawn by venipuncture into acid citrate dextrose (ACD-A, NIH formula A) (1 vol to 5 2/3 WB) in polypropylene tubes (Nalge Co., Rochester, N.Y.) and was centrifuged at 150 x g for 15 minutes at 25°C. The supernatants, consisting of platelet rich plasma (PRP), were pooled from 70 mls of WB. A stable prostacyclin analogue, Iloprost (ZK 36374) [22], was added to platelet-rich plasma at a final concentration of 0.1 μM to minimize activation in the subsequent washing and elutriation procedure. This ZK - treatment did not alter the platelets's responsiveness to ADP when resuspended in ZK-free platelet poor plasma, and incubated at 37°C prior to functional testing. The ZK - treated PRP was adjusted to pH 6.5 with ACD-A and centrifuged at 800 x g for 15 minutes, 25°C. The plasma supernatant was discarded, and the platelet pellets were resuspended in PBS-A buffer containing phosphate buffered saline and albumin (105.5 mM NaCl, 12.8 mM Na_2HPO_4, 2.8 mM KH_2PO_4, 13 mM Na_2EDTA, 15% v:v ACD, 0.5% w:v fatty acid-free bovine serum albumin; 5 M NaOH to titrate pH to 6.5; osmolarity 308 mOsm/l). This platelet suspension was centrifuged at 800 x g for 15 minutes, 25°C. The

supernatant was discarded, and the platelets were resuspended in 4.5 - 5.5 mls of PBS-A, with the platelet count varying from 0.5 to 3.3 x 10^6 platelets/µl. The approximate recovery of platelets from whole blood using this washing procedure was confirmed to be >80% [9].

For reconstituting fractionated platelets with autologous citrated platelet-poor plasma (PPP), WB was drawn into 3.8% citrate (1 vol to 9 vol of blood), centrifuged at 1900 x g for 15 minutes, 25°C. The supernatant PPP was removed, incubated at 37°C for 30 minutes, then kept on ice. The platelet count in PPP was < 1 x 10^4/µl. Prior to use for resuspending pelleted platelet fractions, the PPP was adjusted to pH 7.4 (with ACD-A) and re-incubated at 37°C for 30 minutes.

PLATELET FRACTIONATION

Whole platelet populations were isolated into size dependent fractions by counterflow centrifugation. Also referred to as elutriation, this method of isolation separates cell samples according to size in cell species such as platelets where there is little (< 5 %) variation in density [23]. Platelets were fractionated in a horizontal separation chamber (No. 335205) on an elutriation rotor (No. JE6) and centrifuge (No.J2-21) (All components: Beckman Instruments, Palo Alto, CA). The principle of operation of elutriation is as follows. The platelets introduced are subjected to two opposing forces within the separation chamber: the centrifugal field generated by the spinning rotor, and the counterflow of buffer in the opposite direction. Platelets having different sedimentation rates can be held in suspension. Platelets tend to migrate to a zone where its sedimentation rate is exactly balanced by the flow rate of the buffer through the separation chamber. By

increasing the flow rate of the incoming buffer, successive populations of similarly sized platelets are elutriated from the chamber. Subsequent fractions obtained with higher rates of buffer inflow will contain larger platelets.

The platelets were separated into 9 size-dependent fractions as previously described in greater detail [9]. Briefly, platelets in PBS-A buffer (3.5 to 4.5 mls) were introduced into the separation chamber at 1 ml/minute, a rate at which no platelets are eluted out. The flow rate of incoming buffer was subsequently increased at 1 ml/minute increments for intervals of 2 minutes; one distinct fraction was collected for each interval. Each fraction collected was subsequently counted.

The recovery of platelets introduced into the separation chamber was 86±15 % (± 1 S.D.; range 41-100%), with < 1 % (by number) of contaminating cells, comprising mainly erythrocytes. On 2 occasions, apparent platelet recovery was 41 and 45%, but platelet loss did not appear selective. The size differences and relative numbers of platelets in different fractions at low yields resembled experiments where recovery was > 80 %. In addition, the mean volumes and size histograms for non-elutriated control platelets and those for fractions re-constituted in exact proportion to their yields were not significantly different whether evaluated for a preparation with lower (< 80%) or higher (~100 %) yield. Our general efficiencies of recovery from whole blood was > 70 % ; the mean platelet volumes for the different-sized fractions were within the range as reported by others employing the same isolation technique and claiming an overall platelet recovery from whole blood of ~80% [9,10].

Minimal and comparable activation was observed in all fractions, assessed from quantitative morphometric analyses [24] of platelet shape; all samples used in functional studies contained ~20 % discocytes, ~70% early disco-

echinocytes (DE's; axial ratios were ~0.35 for large or small platelets), and ~10% sphero-echinocytes (SE's). The greater than 90% discocytic platelets which include these early DE's represent essentially "resting-state" platelets which require physiological activators such as ADP or adrenaline for recruitment into aggregates [25].

PLATELET SIZING AND COUNTING

Platelets in PRP or PBS-A buffer (1 volume) were fixed with 0.8 % glutaraldehyde (5 volumes) and counted with an Elzone resistive particle counter (Model 80XY, Particle Data Inc., Elmhurst, Ill.). This device detects as particles, single platelets as well as low order aggregates of platelets by selection between lower and upper size discriminators. The lower size discriminator excludes particles smaller than 1.8 fl; the upper size one excludes 50% of platelet tetramers. Therefore, platelets electronically counted as "single particles" comprise singlets, doublets, triplets and some quadruplets [26]. Operationally, the device counts and sizes particles in isotonic diluent (Hematall) which are flowed through a sensing orifice (48 µm diameter). The movements of particles through the orifice cause changes in electrical impedances (detected by the continuous electrical connection of external and internal electrodes relative to the orifice) which are registered as electrical pulses. These pulses are displayed as counts and are size-associated within the lower and upper size discriminators. Once counts for samples of interest are obtained, they are corrected for background count (< 5% of raw count). No corrections were needed for coincidence as particle counts were < 7000 per 100 µl of diluted suspension counted in ~10 seconds.

Calibration for calculating platelet size was made with

2.02 µm diameter latex particles (Particle Information Services, Bremerton, WA). Calibration was made using a two point calibration line : 4.32 fl corresponded to 2.02 µm particles at one electronic channel, i.e. at channel "54". Two doublings of volume (17.28 fl) corresponded to another channel by addition of doubled electronic channels: "54" + 64 (2 doublings @ 32 channels per doubling) = channel "118". Typical volume histograms for sized fractions and control are shown in Figure 1 for one donor. The mean platelet volumes reported are for electronic volumes which have not been corrected for shape [27]. However, the shape factor is a constant for the different-sized fractions since the morphology distributions were all identical (~80% DE and < 10% SE, with mean thickness and/or diameters the same for all fractions). Therefore, ratios of electronic v values for platelets of different size will be independent of platelet shape. Moreover, the electronic v values and relative ratios reported for the different sized fractions are within ~5% of geometric mean volumes calculated from size and shape measurements of platelets in each fraction by microscopy and, extrapolated to the expected unactivated discocyte population (data not shown).

PLATELET RECONSTITUTION AND FUNCTIONAL STUDIES

The nine collected fractions were pelleted at 1600 x g for 15 minutes, 25°C, and reconstituted as PRP with autologous citrated PPP. To achieve sufficient and comparable numbers of platelets for functional studies in a size dependent fraction, the first three fractions were pooled as the small (S) fraction; the 5th and 6th fractions as the mid-sized fraction (M); and the last two fractions as the large-sized fraction (L). The control fraction was prepared from either: 1) a sample of un-elutriated washed

platelets and reconstituted as PRP in the same way as for the sized fractions, or 2) reconstitution of all elutriated fractions in exact proportion to the platelet mass obtained in each fraction. There was no functional difference between these control types, and data reported on aggregation studies were made on roughly equal numbers of both control types. The reconstituted platelet count (N_o) in any fraction used for functional studies ranged from 74 - 239 x $10^3/\mu l$ in a typical PRP volume of 4 mls.

TURBIDOMETRICALLY-MEASURED SHAPE CHANGE AND AGGREGATION.

Shape change (SC) and macroaggregation (TA) can be measured with an aggregometer, which is a photo-optical device connected to a recording chart. Briefly, PRP is stirred in a glass cuvette, and the light transmission through the turbid sample is recorded. Addition of an aggregating agent causes changes in PRP turbidity associated with platelet activation which alters the pattern of light transmission. Aggregometry tracings were obtained as previously described [28] by using the Payton single channel aggregometer (Payton Associates Ltd., Scarborough, Ont.) with 0 and 100 %T set respectively with light blocked and with water in the cuvette. PRP (0.4 ml) was placed in glass cuvettes (6.9 x 45 mm) with stir bars (6 x 1 mm) and spun at 1000 rpm, 37°C. Aggregating agents were rapidly injected (1 to 10 µl) into stirred PRP with a Hamilton syringe (Hamilton Co., Reno, NV). The rates of change of light transmission (d%T/dt) associated with shape change and macroaggregation were designated as rates of SC (V_s) and TA (V_a), respectively. These were taken as kinetic measurements of SC and TA. The initial rate of decrease in %T following addition of activator parallels the rate of D to DE conversion [24,30]. TA is insensitive to microaggregation,

capable only of measuring the build-up of aggregates containing >10 platelets [19]. The maximal extent of aggregation, %Tmax, was determined as the maximal increase in %T following the initial decrease associated with shape change. The half-time for %Tmax to be reached, $t_{1/2}$(%Tmax), was also determined as a measure of macroaggregation kinetics.

MICROSCOPIC EVALUATION OF PLATELET MORPHOLOGY.

Platelet shape was classified from the appearance of glutaraldehyde-fixed platelets under phase contrast microscopy (40x phase objective on Zeiss Universal Microscope; Carl Zeiss Canada, Montreal, Que.). Criteria used for platelet classification as being discocyte (D), disco-echinocyte (DE) or sphero-echinocyte (SE) were as previously described [24]. Platelet morphology was examined for sized samples fixed under resting conditions to have an idea of 1) the degree of activation resulting from elutriation and plasma resuspension in each sample, and 2) a comparison of the shape factor associated with each sized fraction. Platelet morphology distributions were expressed as the percentage of D, DE and SE in a given sample for at least 300 platelets classified.

Figure 1. Volume histograms for small (S), medium (M) and large (L)-sized elutriated platelets. The log-normal distributions are shown for one donor for similar total numbers of platelets. Means and standard deviations (S.D.) are shown in inset. Control values were respectively 6.4, 4.9 and 8.5 for mean, -1, and +1 S.D. The percent overlap between S and M is 62%; M and L, 56%; and S and L, 27%.

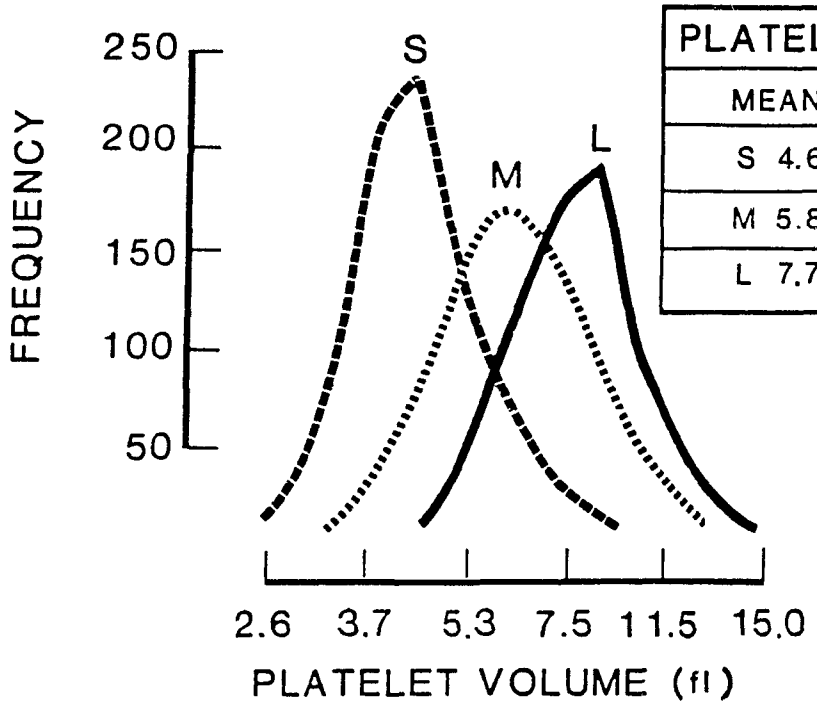

PLATELET VOLUME (fl)		
MEAN	-1 s.d.	+1 s.d.
S 4.6	3.6	6.1
M 5.8	4.7	7.5
L 7.7	6.1	10.0

PLATELET AGGREGATION AND AGGLUTINATION BY PARTICLE COUNTING

Kinetics and sensitivity of aggregation or agglutination were determined by measuring the change in platelet particle number per unit volume with the resistive particle counter at different times following addition of aggregating agent or ristocetin. The percent platelets aggregated or agglutinated, PA_t, was calculated using the relation:

$$\% PA = [1 - (N_t/N_o)] \times 100 \% \quad (1)$$

where N_o, N_t are platelet particle counts respectively at time 0 and t following activator addition [26]. Aggregating agents (1-5 µl) or Ristocetin A (36 µl) were quickly added into stirred PRP (0.1 ml) in an aggregometry cuvette at 37°C. Aggregation or agglutination was arrested by the addition of 0.4 mls of 0.8% glutaraldehyde to the PRP at t ranging from 0 to 30 seconds post addition of aggregating agent or from 0 to 10 seconds for ristocetin. No protein precipitation was seen with ristocetin. These fixed and diluted samples were counted within two hours of fixation. The maximal rate and extent of PA for aggregation were measured respectively at PA_3 (t = 3 seconds corresponding to the initial linear rate of PA) and PA_{10} (referred to as PAmax for t = 10 seconds unless otherwise specified) [19]. The concentration of activator required for half maximal rate or extent of PA, designated as $[Act]_{1/2}$, was obtained for PA at t = 3 to 7 seconds for activator, with some samples of small platelets with slower kinetics best measured at 5 to 7 seconds (so that %PA was > 20-30%), but still corresponding to the initial rate of aggregation. For measurements with ristocetin, the optimal time corresponding

to the initial linear rate was at 5 seconds. The $[Act]_{1/2}$ is a measure of the platelet sensitivity to PA at the initial linear rate of aggregation or agglutination [19].

MATERIALS AND CHEMICALS

Anti-coagulants trisodium citrate and acid citrate dextrose (NIH formula A) were prepared from stock materials purchased from Sigma Chemical Co., St.Louis, Mo., except for fatty acid free bovine serum albumin (ICN Biochemicals, Cleveland, OH). Adenosine diphosphate (ADP), trisodium citrate (all from Sigma Chemical Co.) and glutaraldehyde (8% aqueous stock in sealed ampoules, Polysciences Inc., Warrington, PA) were diluted in Ca^{2+}/Mg^{2+}-free Tyrode's solution (NaCl 140 mM, KCl 2.7 mM, $NaHCO_3$ 0.4 mM; pH 7.4). Iloprost (ZK 36 374; gift from Dr. Th. Krais, Schering AG, Berlin, FRG) was prepared as a frozen 10 µM stock solution in saline (0.9% NaCl and 0.125% sodium bicarbonate, pH 8.2). PAF (purchased from Calbiochem-Behring, La Jolla, CA) was diluted in Tyrode's buffer containing albumin (3.5 mg/ml). U46619 (a stable PGH_2 analogue; gift from Dr. G. Bundy, Upjohn Co., Kalamazoo, MI) was dissolved in 100% ethanol and dissolved in Tyrode's buffer. Ristocetin A (Bio/Data Corp., Hatboro, PA) was reconstituted in distilled water at 15 mg/ml. All agents except for Ristocetin A were added to PRP at < 5% of the total volume.

DATA PRESENTATION:

Rates and extent of aggregation (PA or TA) determined for PRP at varying N_o have not been normalized for N_o unless otherwise specified. Mean ± 1 S.D. are presented for pooled data for different donors, but ratios determined for

different size fractions are based on comparisons for each donor, then averaged except where it is otherwise specified. Tests for significance were made using a Student's t-test determined for paired values for each donor.

RESULTS

AGGREGOMETRIC STUDIES OF LARGE VERSUS SMALL PLATELETS WITH ADP AS ACTIVATOR.

We found using ADP as activator that most samples were responsive to high ADP (10-100 μM), with 10 μM generally yielding 72-90% of maximal values observed at 100 μM ADP for rates of shape change (V_s) and macro-aggregation (V_a). For the samples represented in Table 1, the fractionated platelets were partially refractory to ADP when compared to freshly isolated platelet-rich plasma: 1±0.3 μM and 4.8±0.5 μM for $[ADP]_{1/2}$ causing 50% of maximal rates of change in shape (V_s) and macro-aggregation (V_a) for the different fractions reconstituted in proportion to their respective yields, compared to mean normal values of 0.5 μM and 2-3 μM respectively [19]. This partial refractoriness was readily overcome by increasing ADP as reported for platelets in fresh platelet-rich plasma [19]. We therefore chose to compare maximal functional responses to high ADP (< 100 μM) for the different-sized platelets to ensure that the ADP concentration would not be rate limiting.

Measures of maximal rates of shape change (V_s), macro-aggregation (V_a) and extent of aggregation (%Tmax), made for large vs. small platelets at similar platelet counts (Table 1A), indicate a 2-fold greater functional activity for platelets which were 2-fold larger than the smaller-sized fraction. Similar results have been reported for aggregometric studies using collagen, thrombin and ADP (up to 25 μM)[5,10].

It has been shown previously that turbidometrically-measured parameters are dependent on initial platelet count (N_o), on platelet size (v) and associated geometric cross-section, as well as on platelet refractive index; it was suggested that platelet counts be adjusted to yield platelet suspensions of identical initial turbidity when comparing aggregometrically-measured aggregation [18]. Moreover, we have observed that V_s is approximately constant for No > 200 x $10^3/\mu l$ but decreases by > 50% for N_o at 80-100 x $10^3/\mu l$ (evaluated for unelutriated PRP). We therefore compared aggregometry parameters for large (L) versus small (S) platelets for suspensions having comparable initial light transmission (%T) as shown in Table 1B. This resulted in suspensions with volume fractions actually favouring the smaller platelets (see Table 1B), but this procedure has been reported to minimize any differences in V_s or aggregation parameters other than those related to intrinsic functional differences in L vs. S platelets [18]. Thus, the enhanced responses to ADP observed at similar N_o for the larger sized platelets (Table 1A) generally disappeared at similar initial turbidity (where $\emptyset$ actually favours S platelets) for maximal rates of shape change (V_s) and for rate of macroaggregation (V_a) appears to be significantly enhanced for the small-sized fraction, although the half-time for overall maximal extent of macroaggregation ($t_{1/2}$(%Tmax)) was unaffected by changes in volume fraction, remaining ~2 x elevated for large versus small platelets (compare A and B in Table 1).

Table 1: Shape Change and Macroaggregation (aggregometry) for Large vs Small Platelets With ADP (100 μM) for Varying Platelet Number and Volume Fractions

Fraction	PLATELET PARAMETERS v fl	N_o $x10^3/\mu l$	ϕ $fl/\mu l x10^6$	RESPONSES TO ADP V_s %T/sec	V_a %T/sec	$\%T_{max}$ %	$t_{½}(\%Tmax)$ sec
A) At Similar N_o (7)[a]							
L	7.3 ± 0.1	225 ± 25	1.64	0.72 ± 0.14	0.27 ± 0.17	19 ± 4	72 ± 15
S	4.1 ± 0.1	238 ± 30	0.98	0.48 ± 0.15	0.10 ± 0.03	15 ± 4	126 ± 9
L:S[b]	1.8 ± 0.1**	1.0 ±0.1[+]	1.7±0.3**	1.5 ± .3*	3.5 ± 1.8*	3.2 ±2.3[+]	0.6 ± 0.1*
B) At Similar $\%T_o$ (4)[c]							
L	7.2 ± 0.2	96 ± 10	0.69	0.40 ± 0.20	0.06 ± 0.04	14 ± 5	73 ± 13
S	4.1 ± 0.1	229 ± 6	0.94	0.45 ± 0.25	0.14 ± 0.14	14 ± 7	125 ± 23
L:S[b]	1.8 ± 0.1**	0.4 ±0.1**	0.7±0.1*	1.0 ± 0.5[+]	0.3 ± 0.3[+]	1.3±0.8[+]	0.6 ±0.2*

a Number of donors as shown in brackets, except for the last two columns where only 3 donors' data were used due to low % Tmax values.

b L:S ratios are calculated for each individual donor, and expressed as a mean ± SD for the pooled donors, thereby reducing interdonor variations. Significance of differences shown as $P < 0.01$**; < 0.025*, < 0.10[+]

c The initial light transmission ($\%T_o$) of these PRP were within ~2% of each other (uncorrected $\%T_o$ = 71 ± 5% and 67 ± 5% for L and S respectively).

AGGREGOMETRY STUDIES FOR U46619, PAF AND RISTOCETIN.

Similar results were obtained as reported above for ADP for studies with the stable PGH_2 analogue, U46619, and PAF, when evaluated at similar N_o (Table 2:IA). Rates of shape change and macro-aggregation were respectively ~2 and ~3 fold faster for the large sized platelets compared to the smaller sized ones for U46619 and PAF for comparisons at identical N_o (Data not shown for PAF). Extent of macro-aggregation (%Tmax) and the half-time required to achieve %Tmax also indicated the larger-sized platelets to be more reactive. As in the case for ADP, the enhanced responses of the larger sized platelets to either U46619 or PAF were reduced when tested at similar initial turbidity ($\%T_o$) for L and S platelets (Table 2:IB and II). However, these responses at the lower $\emptyset$ for the large platelets are still 1.5x greater for V_a and %Tmax than for the small platelets, though the scatter in the data is quite large.

Ristocetin-induced agglutination conducted for large and small platelets at varying N_o showed that large platelets agglutinated > 1.5x faster than small platelets for $\emptyset_L > 1.5 \times \emptyset_S$ (n=2), but were equal for equivalent $\emptyset$ (n=1) [data not shown].

MICRO-AGGREGATION KINETICS FOR DIFFERENT-SIZED FRACTIONS AT SIMILAR N_o.

Some preparations that were unusually refractory to ADP when evaluated for aggregometrically-measured aggregation (TA) were consistently very responsive to ADP as measured for early platelet recruitment using particle counting (PA). This was the case for all the different sized fractions.

Table 2: Shape Change and Macro-aggregation Induced by U46619 (100 μm) and PAF for Large vs Small Platelets

Fraction	PLATELET PARAMETERS V fl	N_o $x10^3/\mu l$	$\%T_o$	RESPONSES V_s %T/sec	V_a	%Tmax %	$t_{½}$(%Tmax) secs
I) For U46619 (100 μM)							
A) At Similar N_o (4)[a]							
L	7.2 ± 0.4	192 ± 41	41 ± 11	0.43 ± 0.12	0.34 ± 0.21	22 ± 14	54 ± 9
S	4.2 ± 0.2	204 ± 55	51 ± 13	0.37 ± 0.25	0.16 ± 0.19	12 ± 13	81 ± 38
L:S[b]	1.7 ± 0.1**	1.0 ± 0.2$^+$	0.8±0.1^{++}	1.5 ± 0.6^{++}	3.1 ± 1.3^{++}	2.8 ± 1.3^{++}	0.8±0.3^{++}
B) At Similar $\%T_o$(6)							
L	7.0 ± 0.4	109 ± 35	68 ± 8	0.55± 0.25	0.24 ± 0.9	18 ± 6	60 ± 22
S	4.2 ± 0.1	206 ± 32	66 ± 7	0.64± 0.18	0.16 ± 0.05	14 ± 5	103 ± 14
L:S[b]	1.7 ± 0.2**	0.5 ± 0.2*	1.0 ± 0.1$^+$	0.9 ± 0.3^{++}	1.6 ± 0.6*	1.4 ± 0.6^{++}	0.6 ±0.2^{++}
II) For PAF (1 mg/ml)							
At Similar $\%T_o$ (3)							
L	6.9 ± 0.4	105 ± 29	70 ± 6	0.56 ± 0.23	0.22 ± 0.03	9 ± 4	58 ± 8
S	4.5 ± 0.4	188 ± 59	68 ± 7	0.75 ± 0.25	0.18 ± 0.07	10 ± 7	85 ± 8
L:S[b]	1.6 ± 0.1**	0.6 ±0.1*	1.0 ± 0.0$^+$	0.8 ± 0.2$^+$	2.1 ± 1.1$^+$	1.5 ± 1.3$^+$	0.7 ± 0.1$^+$

a Number of donors as shown in brackets

b L:S ratios individually calculated and expressed as mean ± SD for the pooled donors

Significance of differences shown as $p < 0.01$**; < 0.025*; $< 0.10^{++}$; $> 0.10^+$

The PA time courses showing the maximal initial rates and extents of recruitment for the three size-dependent fractions obtained at similar N_o are shown in Figure 2. This data indicates that the different-sized fractions responded similarly to either 5 or 100 μM ADP, consistent with previous reports of maximal rates of PA in unfractionated PRP achieved with 5 - 10 μM ADP [19,21]. It appears that the larger platelets have greater rates and extents of platelet micro-aggregation. Data on these size-dependent fractions are shown in Table 3 where the larger (L) platelets appear on average 2-3 fold more reactive with respect to recruitment than the smaller (S) platelets for comparisons at similar N_o. The control values (C) shown for non-elutriated platelets are generally intermediate in value, similar in magnitude to the mid-sized fraction, and in the range observed for fresh PRP when determined by electronic counting [26] as reported here, rather than by microscopy [19]. A direct comparison of these parameters for 2 donors for non-elutriated controls versus controls consisting of elutriated platelets reconstituted in direct proportion to platelet mass isolated in each fraction, showed essentially identical results: v respectively = 6.3±0.1 and 6.1±0.2 fl; No = 228±31 x 10^3 and 198±28 x 10^3 /μl; PA_3max = 33±19 and 30±4%, with corresponding $[ADP]_{1/2}$ = 1.7±0.1 and 1.5 μM; and PAmax (at 10 secs) = 45±15 and 55±3%. The half-time for PAmax to be reached, measured for 3 of the donors in Table 2, was 3.5±0.5, 3.6±0.2 and 6.3±0.3 secs for the large, medium, and small platelet fractions respectively, compared to 5.0±2.0 secs for the non-elutriated control. Furthermore, a ratio of each parameter in Table 3 obtained for L vs. S platelets for each donor and then pooled shows L platelets to be 2.5±1.2x and 1.4±0.3x greater than S platelets respectively for PA_3max and PAmax ($p<0.025$ for both); this is associated with a 1.7±0.1 and 1.3±0.2-fold difference respectively in v and ø , but

Figure 2. Kinetics of ADP-induced micro-aggregation (PA) for different sized fractions at comparable initial platelet count (N_o). For large (L: ●), medium (M: ▼) and small (S:■) platelets, the closed symbols are for 5 μM ADP for 3 donors; open symbols for 100 μM ADP for 5 donors, with 2 in common for 5 μM ADP experiments. Symbols represent mean + 1 S.D.(bars). N_o for 5 μM and 100 μM experiments were respectively, 190±25 and 192±29 x $10^3/\mu l$ (Range: 150-237 x $10^3/\mu l$). Mean platelet volumes for these donors are essentially as shown in Table 3A.

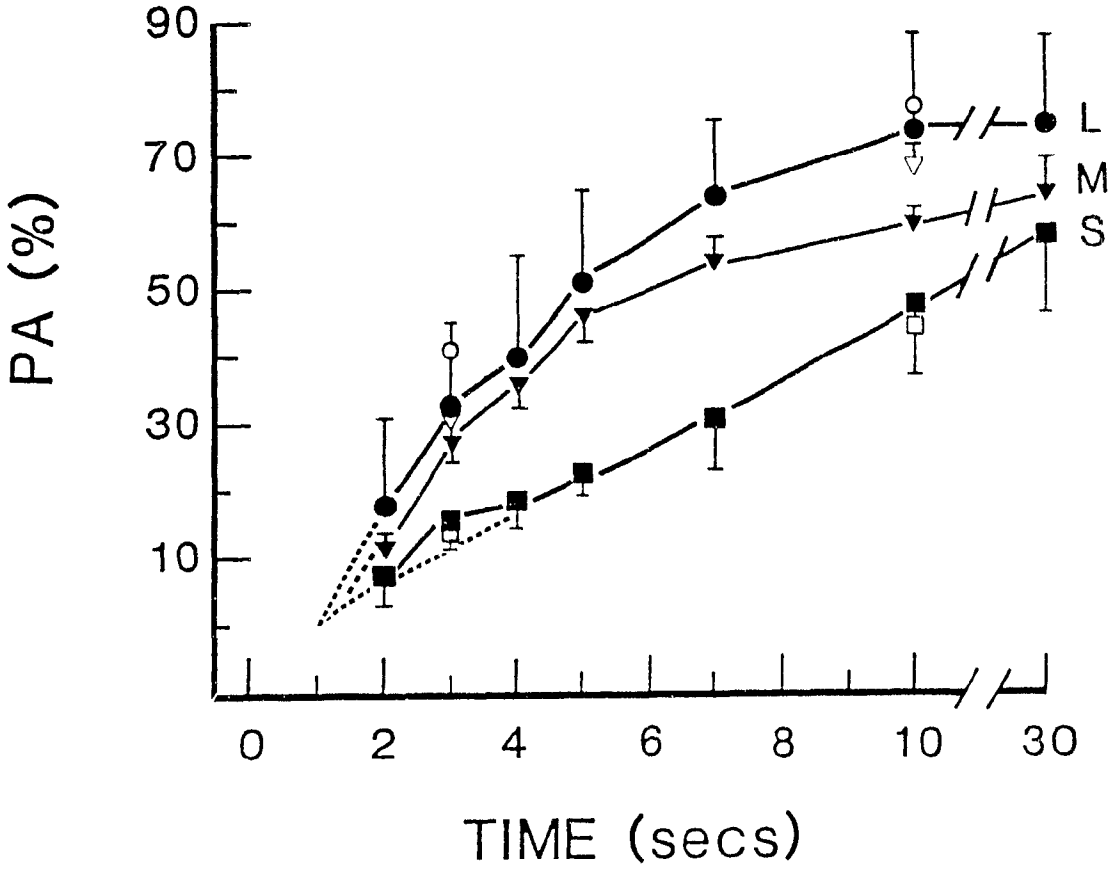

similar N_o (0.9±0.1). Finally, a plot of PA_3max or PAmax values obtained for different PRP at similar N_o against the v for a particular platelet fraction evaluated, shows a highly significant direct linear dependence on v (Figure 3).

PA DEPENDENCE ON INITIAL PLATELET COUNT (N_o)

Given that the different-sized platelets have distinct volume fractions when evaluated at similar N_o, we determined the dependence of the maximal initial rate (PA_3max) and extent (PAmax) on N_o for any given L or S platelet fraction. The linear dependence is most marked for PA_3max and much less so for PAmax, as shown in Figure 4. The regression lines were determined for individual donors for L or S platelet fractions (v values shown in Table 3A) and then represented as an average of these lines in Figure 4; individual regression lines were essentially all parallel. A calculated line ($L(\emptyset_S)$) could then be derived for L platelets yielding PA values corresponding to the volume fraction (v x N_o) equivalent to that for any given N_o for the S platelets (see $L(\emptyset_S)$ lines in Figure 4). Thus, the approximate 2-fold difference in PA_3max values for L versus S platelets is seen to persist for the donors shown in Figure 4. Similar results are shown in Table 3B for the 11 donors evaluated at similar N_o for L versus S platelet fractions where the PA_3 values for L platelets were determined at equivalent $\emptyset$ to that of S platelets for any given donor using the best-fit lines for L platelets shown in Figure 4. For the data in Table 3B analyzed for L:S ratios for individual donors and then pooled, we found up to 2-fold greater values for L vs. S platelets for v (1.7±0.1 ($p < 0.005$)), for PA_3max (2.1±1.2 ($p < 0.05$)) and for $t_{1/2}^{-1}$ for PAmax (1.6±0.5($p < 0.05$)), with considerably smaller differences for PAmax (1.3±0.3($p < 0.05$)).

Figure 3. The dependence of maximal initial rate (PA_3max) and extent (PAmax) of microaggregation (PA) on mean platelet volume (v). Data is shown for PA studies of different-sized fractions at similar N_o (n=5 donors from Table 3A). The r values are correlation coefficients for the linear regression lines ($p < 0.005$ for both r values).

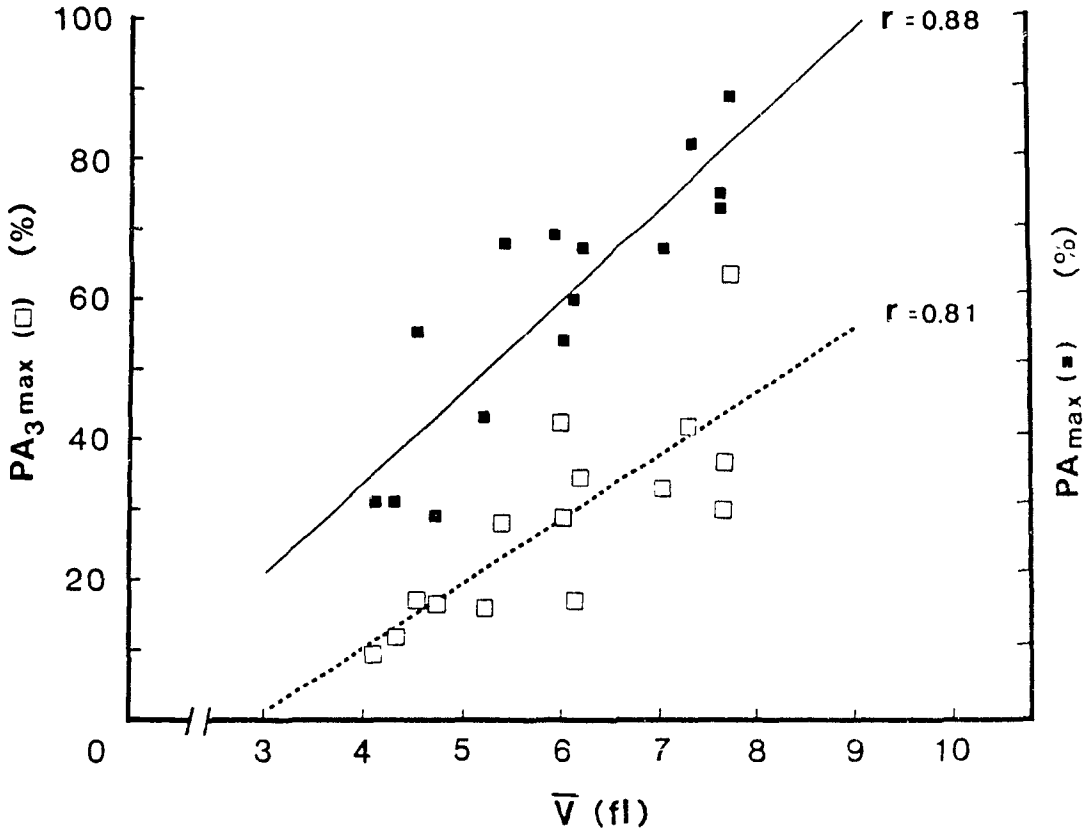

Table 3: Microaggregation (PA) Kinetics for ADP (100μM) for Size-Dependent Fractions Compared at Similar N_0 and at varying Volume Fractions (ϕ).

PLATELET PARAMETERS			RESPONSES TO ADP	
Fraction	V fl	N_0 x $10^3/\mu l$	PA_3max %	PAmax[a]
A) At Similar N_0 (n=11)				
L	7.3 ± 0.2	171 ± 27	41 ± 12	70 ± 9
M	5.9 ± 0.2	184 ± 33	30 ± 12	67 ± 11
S	4.2 ± 0.2	208 ± 20	18 ± 5[b]	53 ± 17
CTL[c]	6.1 ± 0.3	217 ± 40	34 ± 14	70 ± 7[d]
B) At calculated equivalent ϕ (n=11)				
L	7.3 ± 0.2	120 ± 12[e]	37 ± 12	66 ± 9
S	4.2 ± 0.2	208 ± 20	18 ± 5	53 ± 17
C) At ϕ favoring S platelets (n=3)[f]				
L	7.2 ± 0.1	84 ± 5	29 ± 7	76 ± 7
M	5.2 ± 0.2	154 ± 23	23 ± 2	76 ± 12
S	4.0 ± 0.1	229 ± 8	14 ± 4	57 ± 18

a Determined at 10-30 seconds post-activator addition

b Determined at PA_3 for one donor

c n = 9 donors; 4 of the 9 controls were common to L, M, S fractions

d n = 7 donors

e Values are derived from normalization of PA vs N_0 graphs (Fig. 4). These are the N_0 values yielding equivalent ϕ as for the S platelets at N_0 = 208 ± 20 x $10^3/\mu l$

f Mean ϕ are 0.6, 0.8 and 0.9 respectively for L, M and S (SD: ± 7%).

Figures 4A and 4B. Dependence of initial rate (PA_3) and maximal extent (PA_{10}) of aggregation on initial platelet count (N_o). L and S regression lines shown are derived from individual donor regression lines. Distinct symbols represent individual donors (n=7). For 4A, n=4 and 3 donors for L and S fractions respectively; 4B, n=4 and 2 donors for L and S respectively. Lines labelled by $L(\emptyset_S)$ indicate PA responses for L platelets at calculated volume fractions equivalent to that of S platelets. Data for 5 out of 7 donors are shown in Table 3A. Equations for $L(\emptyset_S)$ lines are $y=0.095(x) + 13.3\%$ and $y=0.066(x) + 54.7\%$ for PA_3 and PA_{10} respectively. (Figure shown on next page.)

A

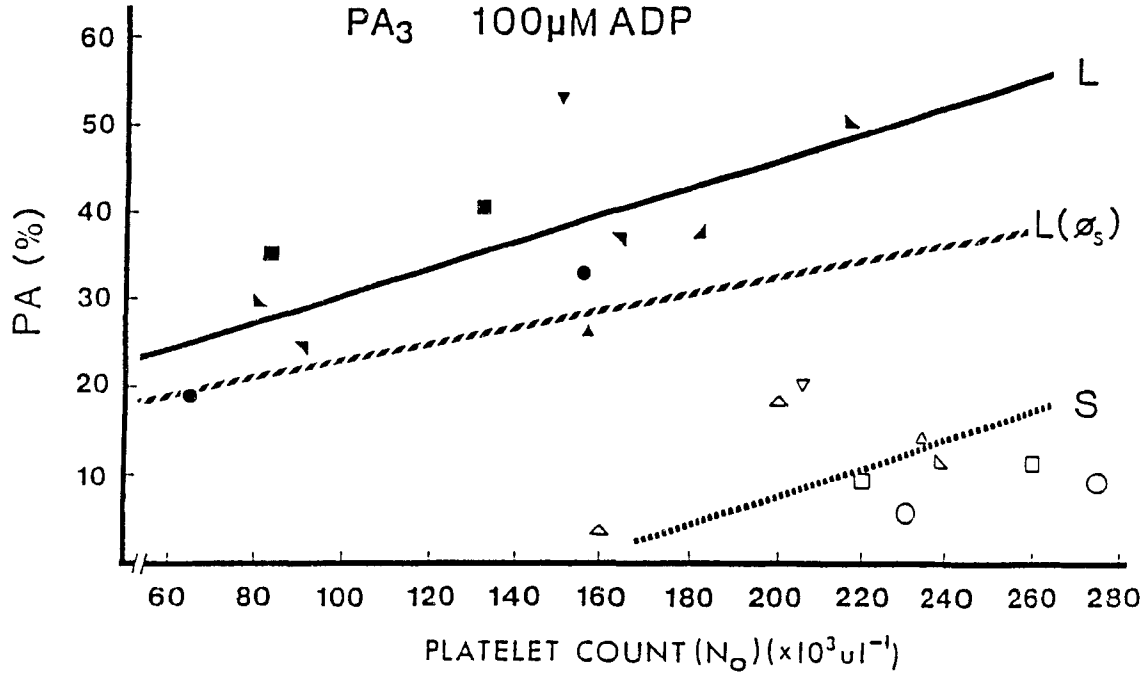
PA3 100μM ADP
PA (%)
60
50
40
30
20
10
L
L(ø_S)
S
60 80 100 120 140 160 180 200 220 240 260 280
PLATELET COUNT (N_o) (×10³ μl⁻¹)

B

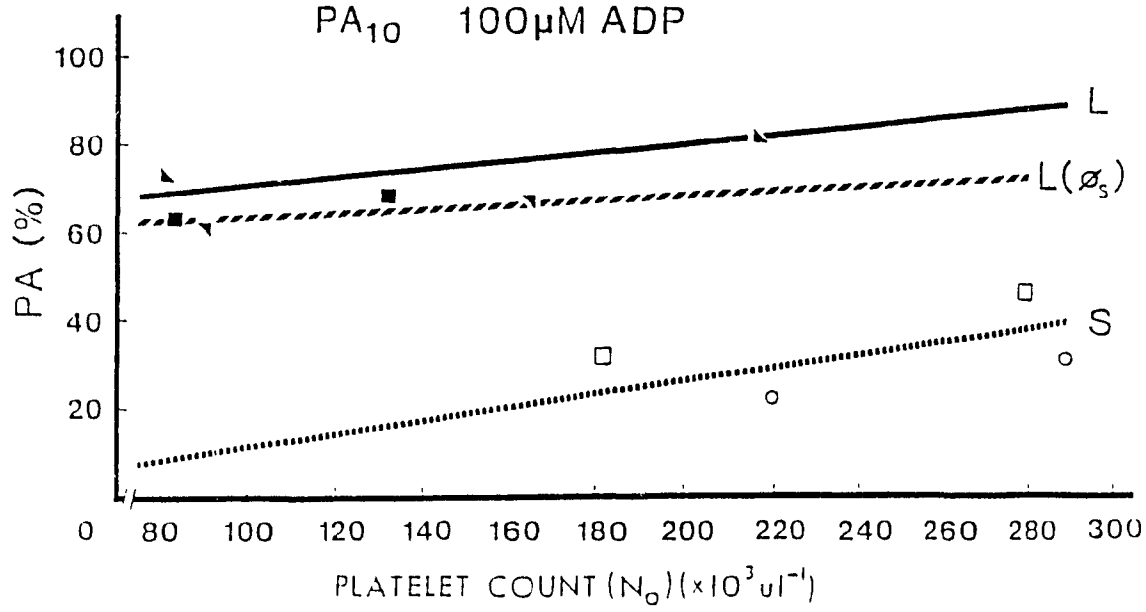
PA10 100μM ADP
PA (%)
100
80
60
40
20
0
L
L(ø_S)
S
80 100 120 140 160 180 200 220 240 260 280 300
PLATELET COUNT (N_o) (×10³ μl⁻¹)

PA AT LOWER N_o AND HIGHER Ø TO FAVOR COLLISION FREQUENCIES OF SMALLER PLATELETS.

The time courses shown in Figure 5 for more comparable platelet volume fractions (Ø) between size-different fractions (lowered N_o for L platelets; data in Table 3B) show similar characteristics as already shown in Figure 2. Back extrapolation of the time courses points to an approximate onset time of ~ 1 second (Figure 5) as previously reported for unfractionated PRP for 10 µM ADP [19]; individual experiments conducted for conditions of low rates of recruitment (PA_3 < 10%) suggest onset times for 5 µM ADP of < 0.5 secs for L, M, and S fractions (see dotted back-extrapolations in Figure 5). Thus, the initial rate of platelet recruitment for large platelets might actually be larger than that reflected by PA_3max, with differences in this parameter under-estimated for large versus small platelets (PA_3max values in Table 3). The larger platelets are more rapidly recruited and to a greater extent than the smaller ones for 5 µM and 100 µM ADP-induced aggregation. The extent of recruitment was comparable for M and L fractions which may be largely attributable to the amount of size overlap between these fractions (~80%), compared to 47±17% between M and S fractions and 27±16% between S and L fractions. Quantitative data is shown for 100 µM ADP in Table 3C. PA kinetics remain distinct for the different-sized fractions, with the L:S fraction responses still favouring platelet rate and extent of recruitment for large platelets in the directions seen in Table 3A and 3B. For the data in Table 3C analysed for L:S ratios for individual donors and pooled, we still observed up to 2-fold greater values for L compared to S platelets for v (1.8±0.1 ($p < 0.01$)) and PA_3max (2.1±0.3 ($p < 0.10$)) with smaller differences for PAmax (1.3±0.3 ($p<0.10$)), all evaluated at

relative volume fractions (0.7±0.1 ($p < 0.2$)) favouring the smaller platelets. The half-times required to reach the above PAmax values were 4.5±0.5, 5.3±1.4 and 7.4±2.3 seconds for the L, M and S fractions respectively, for 3 donors. It appears that larger platelets attain maximal micro-aggregation up to two times more rapidly than the smaller platelets (on average, S:L values for $t_{1/2}$ were 1.6±0.5 ($p < 0.05$)).

Kinetic differences for U46619- and PAF- induced micro-aggregation in the different-sized fractions generally resembled those observed for ADP activation (Table 4). Large platelets were recruited into microaggregates ~1.5 ($p < 0.1$) to ~2 ($p< 0.05$) times more rapidly than small platelets for U46619- and PAF- induced aggregation. As in the case of ADP, mid-sized and control platelets had intermediate responses. The large and mid-sized platelets showed comparable maximal extents of PA for both activators, with somewhat lower values for the smallest platelets (Table 4) as generally observed for ADP (Table 3).

COMPARISONS OF SENSITIVITY AT THE INITIAL RATE OF PA IN DIFFERENT-SIZED FRACTIONS FOR VARYING N_o AND Ø.

Typical log-dose response curves of the initial rate of platelet recruitment for the different sized fractions are shown for a single donor (Fig. 6) and are used to determine ADP sensitivity, i.e., $[ADP]_{1/2}$. PA was typically measured at 3 seconds, but on occasion at 7 seconds for the S platelets, whichever corresponded to the linear initial rate of platelet recruitment. These $[ADP]_{1/2}$ values were so determined for each donor's different sized fractions at similar N_o or Ø with actual mean values reported in Table 5. To effectively compare the relative changes in platelet size with the changes in $[ADP]_{1/2}$ values for the sized fractions,

Table 4: Kinetics for U46619 (100 μM)-and PAF (1 mg/ml)-induced PA at Volume Fractions (♦) favouring Small-Sized Platelets[a]

	PLATELET PARAMETERS		RESPONSES			
	V fl	♦ fl/μlx10⁶	PA, max[b] for U46619 %	PAF	PA max[b,c] for U46619 %	PAF
L	6.9 ± 0.5	0.67 ±0.03	31 ± 9	23 ± 8	72 ± 13	58 ± 10
M	5.2 ± 0.2	0.78 ±0.02	24 ± 4	17 ± 8	68 ± 11	56 ± 9
S	4.1 ± 0.2	0.87 ±0.02	21 ± 11	11 ± 6	58 ± 21	38 ± 22
C	5.4 ± 0.2	0.76 ±0.02	20 ± 8	13 ± 6	70 ± 11	65 ± 24

a Pooled data for 11 donors, of which 9 donors were evaluated for PAF; 7 in common to both.

b Pooled data for 11 and 9 donors respectively for U46619 and PAF.

c PAmax measured at t = 10-30 sec.

Figure 5. Kinetics of ADP-induced PA for different sized fractions at volume fractions actually favouring small platelets. Large (L;○), medium (M;▽) and small (S;□)-sized fractions are shown with closed and open symbols for 5 and 100 uM ADP respectively. Symbols represent mean + 1 S.D. (bars). %PA values for each fraction were normalized to respective average N_o for that sized fraction; v and data for 3 donors are shown in Table 3C. The dashed lines reflect similar onset times of ≤ 0.5 secs found for each of the sized fractions (extrapolated towards 0.5 seconds).

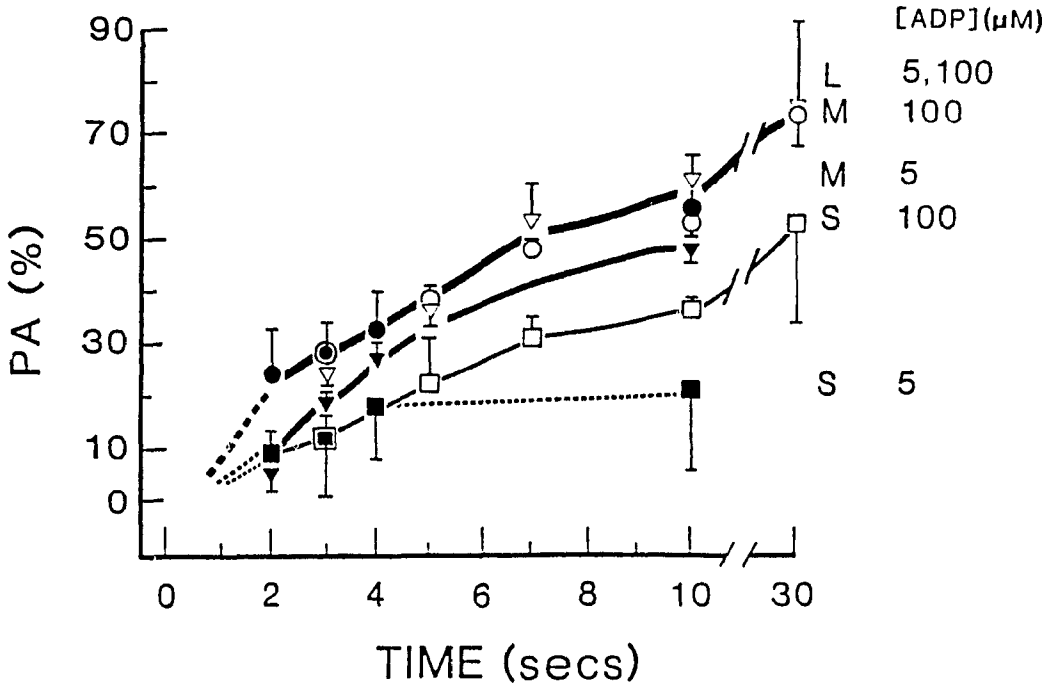

the ratios of the mean values for v and $[ADP]_{1/2}$ were determined individually for each donor and then pooled for eight donors (3 donors from table 3A, 2 donors from Table 3C, one additional donor studied in common for both Tables 3 and 4). Thus, the larger-sized platelets (L) which are on average 1.8±0.3x ($p < 0.01$) larger than smaller-sized platelets (S), are 1.6±0.3x ($p < 0.05$) more sensitive than the S platelets. Identical differences in $[ADP]_{1/2}$ as shown in Table 5 ($p < 0.10$) were obtained for L vs. S platelets for 5 donors evaluated at similar N_o (172±27 and 217±17 x $10^3/\mu l$ respectively for L and S platelets). Comparable ratios of 1.4±0.1 for L:M and M:S mean platelet volume and sensitivity were also observed. Since the measurement of sensitivity, $[ADP]_{1/2}$, has been shown to be independent of platelet count for normal PRP ($N_o > 100,000/\mu l$) [19], the results shown here reflect intrinsic differences in ADP sensitivity of different sized platelets. Indeed, $[ADP]_{1/2}$ appeared independent of platelet volume fractions over the entire range studied ($r = 0.2$, $p > 0.2$ for linear or exponential best fit regression analysis; data not shown).

Sensitivity differences for U46619 and PAF-induced microaggregation were also platelet size-dependent, similar to that found with ADP (Table 5). Typically, large platelets were about 1.5 to 2-fold more sensitive than small platelets for the initial rate of platelet recruitment respectively for U46619 and PAF (both $p < 0.1$). Similar to results for ADP, mid-size and control platelets were found to have intermediate sensitivities for initial recruitment for both U46619 and PAF.

Figure 6. Typical log-dose response curves for control (C) and different-sized fractions (L,M,S) for ADP-induced PA_3 for 1 donor selected from those shown in Table 4.

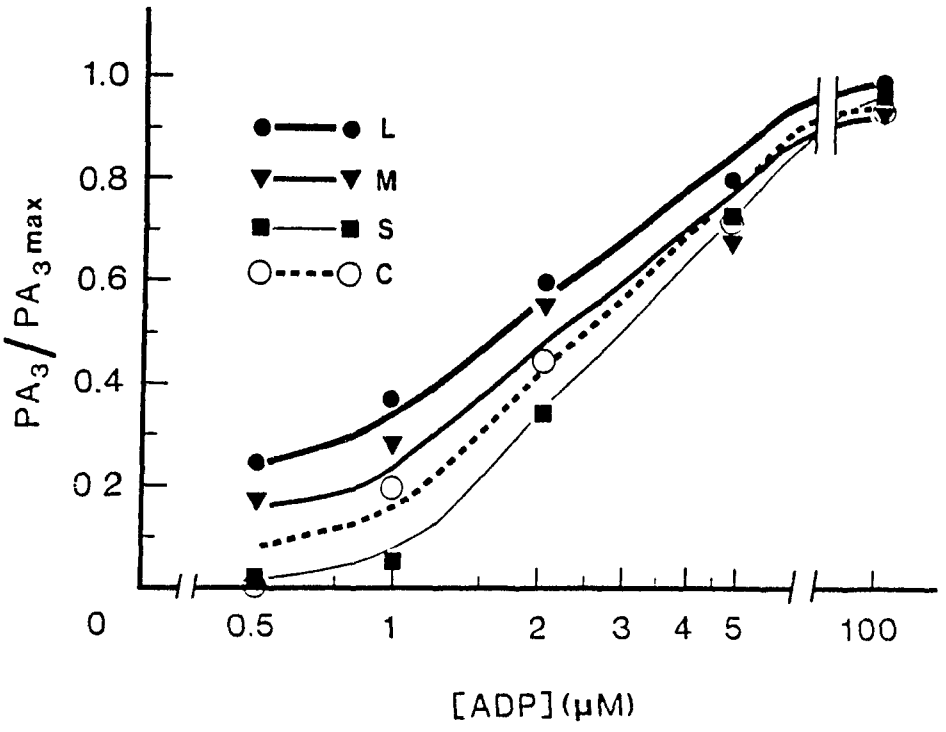

Table 5: Platelet Sensitivity to ADP, U46619 and PAF for Initial Rate of PA as a function of Platelet Size [a]

Platelet Size		[Activator]½ for PA[a]		
	V[b] fl	ADP[c] μM	U46619[d]	PAF[e] ng/ml
L	7.3 ± 0.2	1.2 ± 0.4	1.1 ± 0.6	45 ± 22
M	5.9 ± 0.2	1.5 ± 0.5	1.3 ± 0.6	79 ± 36
S	4.2 ± 0.2	1.9 ± 0.6	1.5 ± 0.5	112 ± 33
C	6.1 ± 0.3	1.6 ± 0.6	1.2 ± 0.5	65 ± 15

a PA determined at t = 3-7 seconds, whichever corresponded best to the initial rate of platelet recruitment.

b Values are for the ADP determinations; actual V values for the other 2 activators determined for 6 and 5 other donors respectively were L = 6.9 ± 0.6, M = 5.2 ± 0.2, S = 4.1 ± 0.2 and C = 5.8 ± 0.3

c n = 8 donors

d n = 6 donors

e n = 3 donors

RISTOCETIN A - INDUCED AGGLUTINATION AT SIMILAR VOLUME FRACTIONS.

The kinetics and sensitivity of platelet recruitment into early aggregates (PA) was evaluated with ristocetin A because it can cause passive, metabolically-independent platelet agglutination and was previously evaluated in size-dependent aggregometric studies [10]. These PA studies were made for different-sized fractions at similar volume fractions to minimize differences in agglutination arising from different collision frequencies associated with varying platelet sizes. The results in Table 6 show essentially identical agglutination sensitivity and comparable rates and extent of recruitment to ristocetin for different-sized platelet fractions. Calculations of L:S values made for each donor and then pooled are similar as values obtained by comparing mean values shown in Table 6; for example, for L:S ratios in v of 1.7±0.2 ($p < 0.05$) corresponding to about equivalent volume fractions (Ø) (1.0±0.4 ($p < 0.4$)), the ratios in sensitivity to ristocetin ($[\text{ristocetin}]_{1/2}$) and in PA_5max values for L:S were essentially unity (respectively 1.0±0.1 and 0.9±0.1 ($p < 0.1$ for both parameters)). Similar identity and significance was obtained in comparing L:M and M:S parameters.

DISCUSSION.

Platelet adhesion to subendothelium and subsequent aggregation are central to the formation of a hemostatic plug in normal hemostasis. The process of aggregation requires normal shape change of unactivated discocytes, leading to rapid recruitment of single platelets into doublets, triplets and multiplets, known as micro-aggregation, with subsequent formation of larger aggregates

Table 6: Ristocetin-Induced Agglutination Kinetics and Sensitivity for Different-Sized Fractions at Similar Volume Fractions[a]

Fraction	PLATELET PARAMETERS V fl	N_0 $x10^3/\mu l$	ϕ $fl/\mu l x10^6$	RESPONSES TO RISTOCETIN $[Ristocetin]^b_{\frac{1}{2}}$ mg/ml	PA_5 max %	PAmax %
L	7.5 ± 0.3	102 ± 31	0.77 ± 0.25	1.4	36 ± 7	91
M	6.4 ± 0.2	127 ± 20	0.81 ± 0.16	1.5 ± 0.1	38 ± 3	81
S	4.5 ± 0.2	186 ± 11	0.83 ± 0.09	1.4 ± 0.1	36 ± 10	77

a 3 donors, except 4 and 1 donor(s) for PA_5 max and PAmax respectively;

b PA at 5 secs with PAmax at 4 mg/ml

referred to as macroaggregation. With certain activators such as ADP, further macroaggregation occurs with associated platelet release. Kinetic studies of these processes with physiological activators clearly indicate that they are sequential in nature, each having distinct sensitivities to activator and inhibitor [19,21]. We have evaluated the relative importance of platelet size and number to these processes, in terms of simple physical differences as well as any intrinsic functional differences associated with the different sized platelets.

Using counterflow centrifugation, we have found that the mean size of circulating platelets in the largest 20% of the population is up to 2-fold that of the smallest 20% of the population, with a parallel enhancement in the large platelets' ability to form platelet aggregates in response to activators. This enhanced efficiency of large platelets over that of small platelets to form aggregates was observed for both the initial microaggregation and more advanced macroaggregation when evaluated at identical platelet numbers (N_o). This physically favors the larger platelet with a higher volume fraction ($\emptyset$).

The first step in platelet activation regulating aggregation is considered to be platelet shape change [25]. Distributions of morphologies in the different sized fractions prior to addition of activator were essentially similar, being ~80% discoidal platelets and less than 10% in the form of advanced sphero-echinocytes (SE). The actual shape factor, i.e., related to the axial ratio (r_p = thickness(t)/diameter(d) < 0.5 for the discoidal platelets) was determined (data not shown) and found to be constant for all the sized fractions. The actual geometric mean volumes for the sized fractions therefore would be 10% to 20% lower than the electronic volumes reported (for r_p = 0.4) [27]. Moreover, the ratios of geometric volumes for the different sized fractions will be identical to those shown for the

mean electronic volumes.

Using high concentrations of activators to minimize any size-dependent differences in platelet sensitivities, we found that maximal rates of shape change were on average independent of platelet size, particularly when determined for platelet suspensions of similar turbidity (Table 1B). Data in Table 1A is complicated by the effects of differences in suspension turbidity on the apparent rate of shape change; it is seen that the apparent maximal rate of shape change can decrease with decreasing platelet number for any given size population. Light scattering artifacts can be minimized by comparing suspensions at similar turbidity (Table 1B), as reported by Holme et al.[18].

All previous studies assessing the dependence of platelet aggregation on platelet size have been conducted for similar platelet numbers for different sized fractions. We have re-confirmed the size dependent differences for macro-aggregation evaluated turbidometrically for large vs. small platelets at similar platelet numbers physically favouring the larger platelets [5,9,10]. In order to dissect out intrinsic platelet functional differences due to size from simple geometric differences favouring larger platelets in aggregation, we evaluated turbidometrically-measured aggregation for the different-sized fractions at equivalent initial turbidity having volume fractions favouring smaller platelets. The advantage of large platelets over smaller platelets for efficient macro-aggregation was thus greatly reduced or eliminated when evaluated at equivalent turbidity for maximal rates (V_a) and extent (%Tmax) of macro-aggregation (Tables 1 and 2). These results are in accord with a report that unfractionated PRP evaluated for normal donors and for donors with abnormally large platelets yielded essentially identical aggregometry curves and rates of macro-aggregation when the different platelet suspensions were compared at identical initial turbidity ($\%T_o$)[18].

Our data thus suggest that L and S platelets show similar V_a and similar TA when initial $\%T_o$ are made comparable for the PRP evaluated. The half time required to achieve the maximal extent of macro-aggregation ($t_{1/2}$(%Tmax)) was found to be up to 2 times shorter for L platelets as compared to S platelets, whether evaluated at similar N_o or $\%T_o$; this parameter appeared independent of platelet count.

The dependence of these aggregation parameters on the $\%T_o$ of PRP was further evaluated by comparing L vs. S platelets at similar $\%T_o$ as in Table 1B for ADP by raising platelet count for S platelets to 520 x $10^3/\mu l$ while maintaining N_o for L platelets at 233 x $10^3/\mu l$. Relative changes in large to small platelets were found as reported in Table 1B for V_s, %Tmax and $t_{1/2}$(%Tmax) (respectively 1.0, 0.9 and 0.6) whereas the relative values for V_a were abnormally high: 1.7 compared to a mean of 0.35 in Table 1B. Thus difficulties in quantitative interpretation of macro-aggregation arise from the large inter-donor variations seen in different parameters evaluated, both for a given size fraction and for the different sized fractions (both Tables 1 and 2), as well as from the complex dependence of light transmission changes on the distributions of macro-aggregate sizes [31].

The difficulties of using light transmission for measuring differences in aggregation behaviour of different sized platelets are further underlined by the observation that the particle optical (light-scattering) efficiency of platelets is about twice as large for L versus S platelets (see Appendix). This suggests that the efficiency of light scatter varies with platelet size, though it would be constant except for variations in platelet refractive index and/or internal structures consistent with a structural heterogeneity in the size-dependent subpopulations.

The above difficulties associated with turbidometric measurements are overcome by direct measurements of initial

platelet recruitment into micro-aggregates using more direct particle counting. These studies showed that large platelets are more sensitive, and are more rapidly recruited than small platelets when evaluated at similar N_o (Tables 3 and 5). That this was only due in part to the simple physical size differences in the platelets was clear from the somewhat reduced but persistent differences in large vs small platelets for aggregation when evaluated at identical volume fraction or at volume fractions favouring S platelets (see Tables 3-5). Large platelets showed up to 3-4 times greater initial maximal rates of PA and up to 2-3 times greater rates for L platelets as compared to S platelets when evaluated respectively at similar N_o and volume fraction. Since relative rates of aggregation under similar collision frequencies are determined by the relative efficiency of collisions [33], it appears that L platelets have about 2-3 fold greater efficiency than S platelets for physiologically induced rates of recruitment into micro-aggregates. In addition, large platelets appear to be up to 2-fold more sensitive than small platelets (Table 5), irrespective of N_o and ϕ . This facilitation of sticky site generation for large platelets would arise from intrinsic differences in membrane surface property of large vs. small platelets.

It appears that PAmax was essentially the same for M and L platelets and was < 30% lower on average for S platelets. This was true whether PAmax was compared at similar N_o (Table 3A) or at ϕ favouring small platelets (Tables 3C and 4). Thus, although the initial rates of PA were up to 2-fold different for L vs S platelets, the final extents of micro-aggregation became comparable. This is consistent with our observations of similar %Tmax for macro-aggregation in all the sized fractions (Tables 1 and 2).

Studies of PA for platelets fractionated by differential aggregation and centrifugation showed "large" platelets to be more sensitive but kinetically slower than "smaller" platelets in their aggregation responses to ADP [11,17]. However, direct comparisons with our results are limited by the large overlap in volume histograms and the use of acid-citrate dextrose as the anticoagulant.

It has been previously reported that different biochemical and functional parameters determined for functionally fractionated platelets at similar platelet numbers correlate positively but, in some cases, non-linearly, with platelet size [11]. We have also observed such variations. Thus, PA_3max and PAmax evaluated at similar N_o varied linearly with platelet size over all fractions studied (Figure 3; $p < 0.005$). However, $[ADP]_{1/2}$ values increased with platelet sizes ($r=0.2$, $p > 0.2$), but not linearly with platelet sizes of the volume fractions evaluated. Better fits could not be obtained by any other curve fitting tests. These analyses may be partially obscured by interdonor variations in any given parameter, such as $[ADP]_{1/2}$. It should be noted that the large (L) and medium (M) fractions had similar overlap in their size histograms as the M and S fractions, namely about 46 - 58% ; overlap between L and S platelets was < 20%.

Platelet shape change is an absolute prerequisite for normal receptor-induced aggregation, as observed with ADP or adrenaline [25], and is associated with membrane and glycoprotein rearrangements leading to fibrinogen binding and aggregation [34,35]. However, ristocetin caused agglutination without any detectable shape change in any of the different sized fractions, as reflected in an unchanged light transmission baseline observed in turbidometric studies reported by others [13,36]. Agglutination measured within 5 seconds of ristocetin addition (Table 6) therefore appears to be a passive, surface-mediated process for all

the size fractions evaluated. Thus the rate, extent and sensitivity for passive agglutination appear essentially identical for all sized fractions, evaluated at similar volume fractions (Table 6) or at similar N_o (data not shown). Since ristocetin-induced agglutination is directly dependent on vWf-VIII multimer binding to glycoprotein Ib (GP Ib) [36], it is expected that the number of GP Ib-associated sticky sites per unit area of platelet may be constant for all sized fractions. This is consistent with our re-calculations of amounts of GP Ib expressed per unit area of plasma membrane from data reported for large, heavy platelets (v ~ 7 fl) and small light platelets (v ~ 3 fl) [37]; this was done using our independent measures of plasma surface area for subpopulations with identical v values (2.7 and 6.8 fl) corresponding to 1.7 fold increase in mean surface area [37].

Intrinsic differences associated with platelet release of dense granules have not been considered in our reported studies as they are not expected to influence the parameters we have chosen for functional studies, namely shape change, $[ADP]_{1/2}$ for V_a, and all PA studies [21]. In addition, although both α- and dense granule content have been reported to increase with platelet size, similar % release was found to occur with platelet activation independent of size [10].

In response to physiological activators, large platelets are predicted to have > 2x the efficiency of generation of plasma membrane sticky sites associated with initial platelet recruitment into aggregates. The most likely source of sticky-site heterogeneity lies in the receptor for Ca^{2+}-fibrinogen binding, namely glycoprotein IIb-IIIa [35]. Studies of platelet size and glycoprotein content have not addressed the question of whether or not larger platelets have intrinsically more glycoprotein per unit area than do smaller ones [37,39-41]. As for

glycoprotein Ib above, we have recalculated amounts of GP IIb-IIIa expressed per unit area of platelet plasma membrane from published data reporting similar amounts per platelet for large versus small platelets [39]. Using our experimental values for mean surface area [38], we find that the larger platelets (v~7fl) contain about one third less glycoproteins IIb and IIIa per unit area of membrane than do the smaller platelets (v~3fl). However, since these glycoproteins must be altered and possibly clustered with platelet activation for expression of fibrinogen-associated sticky sites [34,35]; the relationship of GP IIb-IIIa heterogeneity to dynamics of platelet aggregation and transformation to fibrinogen receptors remains to be elucidated. Further work with flow cytometry on size-dependent subpopulations should help resolve these questions.

The enhanced reactivity of larger platelets representing ~20% of the overall number of platelets present in blood is consistent with reports that < 20-25% of circulating platelets are hemostatically effective [12]. This heterogeneity may arise with platelet production from distinct megakaryocyte precursors [6] and may have clinical importance [15,16,42-44]. For example, a bleeding diathesis is seen less frequently in patients with idiopathic thrombocytopenic purpura or with bone marrow recovery following chemotherapy, with low N_o and high v, than in patients with aplastic anemia with low N_o and low v [16,44]. In so far as PA represents the process of initial platelet hemostasis, large platelets appear to be more sensitive and more rapidly recruitable into aggregates in early hemostatic events. More advanced hemostatic consolidation and/or thrombosis reflected in TA measurements, will also be favoured by participation of larger platelets but largely due to the physical size of the aggregates formed rather than intrinsic biochemical differences. Finally, size-

dependent differences are also being observed in the closely related function of platelet spreading [45].

REFERENCES

1. Corash L, Tan H, Gralnick HR. Heterogeneity of human whole blood platelet subpopulations. I. Relationship between buoyant density, cell volume and ultrastructure. Blood 1977:49;71-87.

2. Frojmovic M M, Milton J G. Human platelet size, shape, and related functions in health and disease. Physiol Rev 1982:62;185-261.

3. Karpatkin S: Heterogeneity of human platelets I. Metabolic and kinetic evidence suggestive of young and old platelets. J Clin Invest 1969:48;1073-1082.

4. Karpatkin S. Heterogeneity of human platelets. II. Functional evidence suggestive of young and old platelets. J Clin Invest 1969:48;1083-1087.

5. Karpatkin S. Heterogeneity of human platelets. VI. Correlation of platelet function with platelet volume. Blood 1978:51;307-316.

6. Penington D G, Streatfield K, Roxburgh A E. Megakaryocytes and the heterogeneity of circulating platelets. Br J Haematol 1976:34;639-653.

7. Penington D G, Lee N L Y, Roxburgh A E, McGready J R. Platelet density and size: The interpretation of heterogeneity. Br J Haem 1976:34;365-376.

8. Leone G, Agostini A, DeCrescenzo A, Bizzi B. Platelet heterogeneity: relationship between buoyant density, size, lipid peroxidation and platelet age. Scand J Haem 1979:23;204-210.

9. Thompson C B, Eaton K A, Princiotta S M, Rushin C A. Valeri C R. Size dependent platelet subpopulation relationships of platelet volume to ultrastructure enzymatic activity and function. Brit J Haematol 1982:50;509-519.

10. Thompson C B, Jakubowski J A, Quinn P G, Deykin D, Valeri C R. Platelet size as a determinant of platelet function. J Lab Clin Med 1983:101;205-213.

11. Carty D J, Gear A R L. Fractionation of platelets according to size: functional and biochemical characteristics. Am J Haem 1986:21;1-6.

12. Schulman N R, Watkins S P, Itscoitz S B, Students A B. Evidence that the spleen retains the youngest and hemostatically most efficient platelets. Trans Assn Am Physicians 1969:81;302-313.

13. Thompson C B, Jakubowski J A, Quinn P G, Deykin D, Valeri C R. Platelet size and age determine platelet function independently. Blood 1984:63;1372-1375.

14. Thompson CB: Selective consumption of large platelets during massive bleeding. Br Med J 1985:291;95-96.

15. Savage B, McFadden P P, Hanson S R, Harker L A. The relation of platelet density to platelet age: survival of low- and high density ^{111}Indium-labeled platelets in baboons. Blood 1987:68;386-393.

16. Harker L A, Slichter S J. The bleeding time as a screen test for evaluation of platelet function. N Eng J Med 1972:287;155-159.

17. Haver V M, Gear A R L. Functional fractionation of platelets: aggregation kinetics and glycoprotein labelling of differing platelet populations. Thrombos Haemost 1982:48(2);211-216.

18. Holme S, Simmonds M, Ballek R, Murphy S. Comparative measurements of platelet size by Coulter Counter, microscopy of blood smears, and light transmission studies. J Lab Clin Med 1981:97;610-622.

19. Frojmovic M M, Milton J G, Duchastel A. Microscopic measurements of platelet aggregation reveal a low ADP-dependent process distinct from turbidometrically measured aggregation. J Lab Clin Med 1983:101;964-976.

20. Gear A R L, Lambrecht J K. Reduction in single platelets during primary and secondary aggregation. Thrombos Haemost 1981:45;298.

21. Pedvis L G, Wong T, Frojmovic M M. Differential Inhibition of the platelet activation sequence: shape change, micro- and macro-aggregation, by a stable prostacyclin analogue (Iloprost). Thrombos Haemost 1988:59;323-328.

22. Schor K, Darius H, Matzky R, Ohlendorf R. the antiplatelet and cardiovascular actions of a new carbacyclin derivative (ZK 36374)-equipotent to PGI_2 in vitro. Arch Pharm 1981:316;252-255.

23. Lindahl P E. Principle of a counter-streaming centrifuge for the separation of particles of different sizes. Nature 1948:16;648-649.

24. Frojmovic M M, Milton J G. Physical, chemical and functional changes following platelet activation in normal and "giant" platelets. Blood Cells 1983;9:359-382.

25. Milton J G, Frojmovic M M. Adrenaline and adenosine diphosphate-induced platelet aggregation require shape change. J Lab Clin Med 1984:104;805-815.

26. Frojmovic M M, Milton J G, Gear A L. Platelet aggregation measured in vitro by microscopic and electronic particle counting. In: Methods in Enzymology. Vol. 169, Hawiger J, Coloswick S P, Kaplan N O (eds.). Academic Press 1988. (In Press)

27. Milton J G, Yung W, Frojmovic. Dependence of platelet volume measurements on heterogeneity of platelet morphology. Biophys J 1981:35;257-261.

28. Frojmovic M M, Panjwani R: Blood cell structure-function studies: light transmission and attenuation coefficients of suspensions of blood cells and model particles at rest and with stirring. J Lab Clin Med 1975:86;326-343.

29. Tang S S, Frojmovic M M. Inhibition of platelet function by antithrombotic agents which selectively inhibit low-Km cyclic 3',5'-adenosine monophosphate phosphodiesterase. J Lab Clin Med 1980:95;241-257.

30. Milton J G, Frojmovic M M. Turbidometric evaluations of platelet activation: relative contributions of measured shape change, volume, and early aggregation. J Pharmacol Met 1983:9;101-115.

31. Nichols A R, Bosmann H B. Platelet aggregation: newly quantified using nonempirical parameters. Thrombos Haemost 1979:42;679-693.

32. Holme S, Murphy S. Influence of platelet count and size on aggregation studies. J Lab Clin Med 1981:97;623-630.

33. Chang H N, Robertson C R. Platelet aggregation by laminar shear and Brownian motion. Ann Biomed Eng 1976:4;151-183.

34. Oliver J A, Albrecht R M. Colloidal gold labelling of fibrinogen receptors in epinephrine- and ADP- activated platelet suspensions. Scanning Microsc 1987:1;745-756.

35. Nurden A T. Platelet membrane glycoproteins and their clinical aspects. In: Thrombosis and Hemostasis 1987. Verstraete M, Vermylen J, Lijnen R, Arnout J (eds.), pp 93-125. Leuven University Press, Leuven, Belgium 1987.

36. Ruan C G, Du X P, Xi X D, Castaldi P A, Berndt M C. A murine antiglycoprotein Ib complex monoclonal antibody, SZ 2, inhibits platelet aggregation induced by both ristocetin and collagen. Blood 1987:69;570-577.

37. Adelman B, Michelson A D, Handin R I, Ault K A. Evaluation of platelet glycoprotein Ib by fluorescence flow cytometry. Blood 1985:66;423-427.

38. Frojmovic M M, Milton J G, Wong T. Platelet subpopulations: external to invaginated plasma membrane surface area is constant, independent of size. Thrombos Res Suppl 1986:IV;119.

39. Johnston G I, Hepinstall S, Robins R A, Price M R. The expression of glycoproteins on single blood platelets from healthy individuals and from patients with congenital bleeding disorders. Biochem Biophys Res Comm 1984:123;1091-1098.

40. Nomura S, Nagata H, Oda K, Kokura T, Yasumaga K. Effects of EDTA on the membrane glycoproteins IIb-IIIa complex: analysis using flow cytometry. Thrombos Res 1987:47;47-58.

41. Michelson A D. Flow cytometric analysis of platelet surface glycoproteins: phenotypically distinct subpopulations of platelets in children with chronic myeloid leukemia. J Lab Clin Med 1987:110;346-354.

42. Bessman J D, Williams L J, Gilmer P R. Platelet size in health and hematological disease. Am J Clin Path 1982:78;150-153.

43. Bessman J D, Gilmer P R, Gardner F H. Use of mean platelet volume improves detection of platelet disorders. Blood Cells 1985:11;127-135.

44. Garg S K, Amorosi E L, Karpatkin S. Use of the megathrombocyte as an index of megakaryocyte number. N Engl J Med 1971:284;11-17.

45. Frojmovic M M, Wong T, Timm M. Spreading and early aggregation for large versus small platelets. Thrombos Haemost 1985:54;247.

CHAPTER III

JOINT SUMMARY AND CONCLUSIONS.

The relative contributions of platelet size (v), platelet number (N_o), and platelet volume fraction ($\emptyset$) to platelet shape change and aggregation kinetics and sensitivity were assessed for different-sized subpopulations. This study points out the relative importance of these parameters and their interplay in the evaluation of platelet activation in light of the following observations:

A) Turbidometric measurements:

1) Measures of maximal rates of shape change (V_s), macroaggregation (V_a) and extent of aggregation (%Tmax), made for large vs. small platelets at similar N_o, indicate 2-fold greater functional activity for platelets which were 2-fold larger than the smaller sized fraction. This is consistent with other studies which have obtained similar size-dependent results for aggregometric studies using collagen, thrombin and ADP.

2) The enhanced responses to ADP observed at similar N_o for the larger sized platelets generally disappeared at similar initial turbidity ($\%T_o$) (where $\emptyset$ actually favours S platelets) for maximal rates of shape change and for extent of macroaggregation (%Tmax). At similar $\%T_o$, the initial rate of macroaggregation (V_a) appears to be significantly enhanced for the small-sized fraction, although the half-time for overall maximal extent of macroaggregation ($t_{1/2}$(%Tmax)) was unaffected by changes in volume fraction, remaining ~2 x elevated for large versus small platelets.

3) For studies with the stable PGH_2 analogue, U46619, and platelet activating factor, PAF, rates of shape change and macroaggregation were respectively ~2 and ~3 fold faster for the large sized platelets compared to the smaller sized ones for comparisons at identical N_o. Extent of macroaggregation (%Tmax) and the half-time required to achieve %Tmax also suggested the larger-sized platelets to be more reactive. As for ADP, the enhanced responses of the larger sized platelets to either U46619 or PAF were reduced when tested at similar initial turbidity ($\%T_o$).

4) Ristocetin-induced agglutination measured turbidometrically as macroaggregation (TA) for large and small platelets at varying N_o showed that large platelets agglutinated at rates paralleling the volume fraction advantage over S platelets. Thus agglutination rates for L and S platelets were equal for equivalent ø.

B) Particle Counting

1) Large (L) platelets appear on average 2-3 fold more reactive to ADP, U46619, and PAF with respect to microaggregation (PA) than the smaller (S) platelets for comparisons at similar N_o. The control values (C) for non-elutriated platelets are generally intermediate in value, similar in magnitude to the mid-sized fraction.

2) A plot of PA_3max or PAmax values obtained for size-dependent fractions at similar N_o against the v for the particular platelet fraction evaluated, shows a highly significant direct linear dependence on v. This linearity was not always continuous from S to M to L platelets.

3) The linear dependence of the maximal initial rate (PA_3max) on N_o for any given L or S platelet fraction was more marked than for PAmax.

4) PA kinetics in response to ADP at ϕ favoring collision frequencies of smaller platelets remained distinct for the different-sized fractions, with the L:S fraction responses still favouring platelet rate and extent of recruitment for large platelets in the directions seen at similar N_o or equivalent ϕ. Kinetic differences for U46619- and PAF- induced PA in the different-sized fractions generally resembled those observed for ADP activation.

5) Comparisons of sensitivity ($[activator]_{1/2}$) at the initial rate of PA in different-sized fractions for varying N_o and ϕ showed L platelets to be more sensitive than S platelets by up to 2 fold. The $[activator]_{1/2}$ appeared to be independent of platelet volume fraction. Sensitivity differences for U46619- and PAF-induced microaggregation were also platelet size-dependent, similar to that found with ADP. Typically, large platelets were about 1.5 to 2-fold more sensitive than small platelets for the initial rate of platelet recruitment; mid-size and control platelets were found to have intermediate sensitivities.

6) Essentially identical agglutination sensitivities and comparable rates and extent of microaggregation (PA) induced by ristocetin were found for the different-sized platelet fractions. The kinetics and sensitivity of PA was evaluated with ristocetin because it can cause passive, metabolically-independent platelet agglutination.

Conclusions:

Evidence already exists to support the concept of platelet functional heterogeneity. This study confirms that idea and emphasizes the need to appreciate certain variables in the interpretation of measures of platelet aggregation. Based on the preceding observations, the following conclusions are drawn:

1) Using counterflow centrifugation, we have found that the mean size of circulating platelets in the largest 20% of the population is up to 2-fold that of the smallest 20% of the population, with a parallel enhancement in the large platelets' ability to form platelet aggregates in response to activators. This enhanced efficiency of large platelets over that of small platelets to form aggregates was observed for both the initial micro-aggregation and more advanced macroaggregation when evaluated at identical platelet numbers (N_o), which physically favours the larger platelet with a higher volume fraction ($\emptyset$).

2) Previous studies assessing the dependence of platelet aggregation on platelet size have been conducted for similar platelet numbers for different sized fractions. We have re-confirmed the size dependent differences for macro-aggregation evaluated turbidometrically for large vs. small platelets at similar platelet numbers physically favouring the larger platelets. In order to dissect out intrinsic platelet functional differences due to size from simple geometric differences favouring larger platelets in aggregation, turbidometrically-measured aggregation was evaluated at equivalent initial turbidity having volume fractions favouring smaller platelets. The advantage of large platelets

over smaller platelets for efficient macroaggregation was thus greatly reduced or eliminated when evaluated at equivalent turbidity for maximal rates (V_a) and extent (%Tmax) of macroaggregation. Platelet volume fractions and $\%T_o$ must also be adjusted for determinations of platelet size-dependent shape change kinetics when using turbidometry but not for microscopic methods.

3) Difficulties in quantitative interpretation of macro-aggregation arise from the large inter-donor variations seen in different parameters evaluated, both for a given size fraction and for the different sized fractions, as well as from the complex dependence of light transmission changes on the size dependent optical efficiencies for individual platelets (see Appendix) and on the distributions of macro-aggregate sizes.

4) The difficulties associated with turbidometric measurements are overcome by direct measurements of initial platelet recruitment into micro-aggregates using particle counting. These studies showed that large platelets are more sensitive, and are more rapidly recruited and to a greater extent than small platelets when evaluated at similar N_o. That this was only due in part to the simple physical size differences in the platelets was clear from the reduced but persistent differences in large vs small platelets for aggregation when evaluated at identical volume fraction or at volume fractions favouring S platelets. Since relative rates of agggregation under similar collision frequencies are determined by the relative efficiency of collisions, it appears that L platelets have about 2-3 fold greater efficiency than S platelets

for physiologically induced rates of recruitment into micro-aggregates. In addition, large platelets appear to be up to 2-fold more sensitive than small platelets, irrespective of N_o and ϕ .

5) In so far as PA represents the process of initial platelet hemostasis, large platelets appear to be more sensitive and more rapidly recruitable into aggregates in early hemostatic events. More advanced hemostatic consolidation and/or thrombosis reflected in TA measurements, will also be favoured by participation of larger platelets but largely due to the physical size of the aggregates formed rather than intrinsic biochemical differences.

6) Optical (or light scattering) efficiencies (k) are size-dependent within a whole platelet population. Typically, for large versus small platelets of 2-fold difference in size, the difference in k is greater for the large platelets by same factor. In addition, $\%T_o$ are not identical between large versus small platelets compared at similar platelet volume fractions because of the dissimilarity in k values. This likely reflects differences in refractive index associated with internal structures and/or membrane for large versus small platelets.

7) Some biochemical and functional parameters may correlate positively but, in some cases, non-linearly, with platelet size. We have also observed such variations. Specifically, PA_3max and PAmax evaluated at similar N_o varied linearly with platelet size over all fractions studied. However, $[ADP]_{1/2}$ values correlated positively but not linearly with platelet sizes of the volume fractions evaluated.

8) The rate, extent and sensitivity for passive agglutination appear essentially identical for all sized fractions, evaluated at similar volume fractions or at similar N_o. Since ristocetin-induced agglutination is directly dependent on vWf-VIII multimer binding to glycoprotein Ib (GP Ib), it is expected that the number of GP Ib-associated sticky sites per unit area of platelet may be constant for all sized fractions.

9) In response to physiological activators such as ADP, U46619 and PAF, large platelets are predicted to have up to 2x the efficiency of generation of plasma membrane sticky sites associated with initial platelet recruitment into aggregates. The facilitation of sticky site generation for large platelets would arise from intrinsic differences in membrane surface property of large versus small platelets. The most likely source of sticky-site heterogeneity lies in the expression of new receptors for Ca^{2+}-fibrinogen binding, namely glycoprotein IIb-IIIa.

10) The enhanced reactivity of larger platelets representing ~20% of the overall number of platelets present in blood is consistent with reports that < 20-25% of circulating platelets are hemostatically effective. This heterogeneity may arise with platelet production from distinct megakaryocyte precursors and may have clinical importance.

FUTURE STUDIES IN PLATELET SUBPOPULATIONS.

Other experimental approaches have been used to study platelet subpopulations. Flow cytometry, for example, is a technique in which individual cells are passed in a fluid stream and are analysed by sensors which measure specific physical or chemical characteristics of these cells. The parameters studied may reflect structural (e.g., cell size and shape) or functional (e.g., surface receptors) characteristics [1]. One particular feature of flow cytometry, cell sorting, uses electrical or mechanical means to screen out cells with preselected characteristics from the main analytical stream, and thus can yield cells with more homogeneous characteristics. With respect to platelets, the analysis of surface glycoproteins using flow cytometry is ideal because of: 1) the low numbers of platelets actually needed for testing; 2) the ability to detect and sort out subpopulations; and 3) simultaneous platelet size measurement. It is becoming widely used as a diagnostic and experimental tool in the study of hematological disorders [2,3]. Flow cytometry studies have suggested that large platelets contain more GP IIb-IIIa than small platelets [4]. Moreover, there may be a direct relationship between platelet size and the number of surface glycoproteins per platelet. However, it is uncertain whether large platelets intrinsically have more GP IIb-IIIa, i.e., amounts of glycoprotein per unit surface area. The analysis of glycoprotein characteristics on platelet subpopulations must therefore correct for platelet surface area.

Another focus of future study may be on the dynamics of glycoprotein expression on the platelet membrane. For example, the rate at which GP IIb-IIIa is surface-expressed or clustered may be different amongst size-dependent platelets. Intracellular events associated with platelet activation are likely to reflect functional differences

observed in subpopulations. The dynamics of Ca^{2+} movements are closely linked with physiological activation, and can be monitored with markers such as FURA or Quin-2 in parallel with aggregation/activation studies [5,6]. The focus of further studies should be towards the elucidation of membrane-related mechanisms in activation, which these present studies suggest appears to mediate platelet functional heterogeneity.

REFERENCES

1. Shapiro H. What is flow cytometry ?. In:Practical Flow Cytometry. Alan R. Liss Inc., New York 1985.

2. Michelson A D. Flow cytometric analysis of platelet surface glycoproteins: phenotypically distinct subpopulations of platelets in children with chronic myeloid leukemia. J Lab Clin Med 1987:110;346-354.

3. Adelman B, Michelson A D, Handin R I, Ault K A. Evaluation of platelet glycoprotein Ib by fluorescence flow cytometry. Blood 1985:66;423-427.

4. Nomura S, Nagata H, Oda K, Kokura T, Yasumaga K. Effects of EDTA on the membrane glycoproteins IIb-IIIa complex: analysis using flow cytometry. Thrombos Res 1987:47;47-58.

5. Rink T J, Smith S W, Tsien R Y. Cytoplasmic free Ca^{2+} in human platelets: Ca^{2+} thresholds and Ca-independent activation for shape-change and secretion. FEBS Letters 1982:148;21-26.

6. Grynkiewicz G, Poenie M, Tsien R Y. A new generation of Ca^{2+} indicators with greatly improved flourescence properties. J Biol Chem 1985:260;3440-3450.

APPENDIX

PLATELET OPTICAL DENSITY PER UNIT SURFACE AREA DEPENDS ON PLATELET SIZE.

Introduction:

The optical density (or extinction (e)) of a cell population reflects its light scattering properties and is influenced by parameters such as cellular refractive index (n_r), size, shape and internal structures. These factors typically determine the initial light transmission ($\%T_o$) of unactivated platelet-rich suspensions. From theoretical calculations [1-4], it is predicted that normal platelets would have similar optical efficiencies (k; = extinction per unit cross-sectional surface area), regardless of the mean platelet volume of the population if overall shape, internal structures and n_r are the same.

The parameter e is more closely related to the platelet cross-sectional surface area rather than its volume, and is therefore expected to be constant if it is expressed per unit platelet cross-sectional area (i.e., as k) instead of per unit volume. Here, the dependence of e on the relative cross-sectional area of platelets (expressed as $v^{2/3}$), was examined for different-sized platelets in normal donors. The results suggest a dependence of k on platelet size within a normal platelet population.

Methodology:

For the preparation of platelet-rich plasma (PRP) and platelet-poor plasma (PPP), the isolation of size-dependent platelet subpopulations, and the determination of platelet electronic volume (v), refer to Chapter II, " Methods and Materials ".

Measurement of light transmission (%T)

Light transmission (%T) of PRP and PPP suspensions was obtained using a Payton single channel aggregometer (Payton Associates Ltd., Scarborough, Ont.) with 0 and 100 %T set respectively with light blocked and with water in the cuvette. PRP or PPP (0.4 ml) was placed in glass cuvettes (6.9 x 45 mm) with stir bars (6 x 1 mm) and spun at 1000 rpm, 37 C. Aggregometer settings and further experimental details were exactly as previously described [1,2]. The PPP was used instead of platelet-free plasma (PFP)[2] as it contained < 5% of the platelets present in PRP and gave $\%T_o$ within ~1% transmission units of that observed with PFP [2].

Theoretical Background:

Platelets behave as light scattering particles described by the Beer-Lambert law:

$$E_\gamma^\lambda = -\log T_\gamma^\lambda = K_\gamma^\lambda N L \qquad (1)$$

Where E_γ^λ and T_γ^λ are respectively, the optical density and transmission of the suspension, at a wavelength λ and optical geometry γ ; N = the particle concentration (number per milliliter); L=light path length of the glass cuvette (in centimeters); K_γ^λ = the particle attenuation coefficient for λ and γ(in square centimeters) which are respectively, the components due to absorption and scattering by the light-particle interactions; and γ = the half-angle subtended at the sample by the axial light detector.

In the case of platelets in PRP,

$$E_{plts} = E_{PRP} - E_{PPP} = K_{\gamma}^{\lambda} N\ L \qquad (2)$$

where E_{plts} = the optical density or extinction of the platelets, E_{PRP} and E_{PPP} are respectively, the extinctions measured in platelet-rich plasma and platelet-poor plasma. In addition,

$$K_{\gamma}^{\lambda} = \frac{E_{\gamma}^{\lambda}}{N\ L} = \frac{e}{L} \qquad (3)$$

where e = extinction per platelet. The particle (or platelet) optical efficiency is defined by:

$$k = \frac{K_{\gamma}^{\lambda}}{0.434\ A} \qquad (4)$$

where A, the particle projected area = πa_s^2 with a_s represented by the radius of a spherical particle or of an equivalent sphere for an axi-symmetric particle, based on the average particle volume ($v = 4/3\pi a_s^3$). Therefore, by combining equations (3) and (4), we obtain:

$$k = \frac{e}{0.434\ (3v/4\pi)^{2/3}\ L} \qquad (5)$$

With rearrangement, equation (5) becomes:

$$\frac{e}{v^{2/3}} = b \cdot k = k' \qquad (6)$$

where $b = 0.434L(3/4\pi)^{2/3}$, and is a constant fixed for a given cuvette geometry, and k'= the apparent k for a given cuvette.

From the above, it is expected that a plot of e versus $v^{2/3}$ for platelets of different sizes will yield a straight line with a zero intercept to indicate a proportional relationship of extinction per platelet (e) and platelet cross-section. However, it would also indicate an overall similar refractive index and distribution of platelet internal structures between different-sized platelets.

Results:

Figure A shows the dependence of e on platelet cross-sectional area. There appears to be a size dependence of extinction per unit surface area as the line does not pass through zero. Large (L) platelets display about twice the optical efficiency of small (S) platelets. Data for Figure A is shown in Table A. For mid-sized (M) and reconstituted control (C) platelets, the optical efficiencies are similar and are intermediate between L and S platelets. The differences in k' appear to parallel the differences in platelet size (Table A).

Discussion:

Differences in optical efficiency between sized fractions may be related to intrinsic platelet characteristics [1-3]. This is consistent with observations that these same sized fractions display different biochemical and functional capacities. It is observed that $\%T_o$ is not identical for large-(L) versus small-(S) sized platelet suspensions compared at similar volume fractions. Differences between L and S platelets with respect to intracellular content and structure (e.g., granular content and/or distribution) would alter platelet optical efficiency [1,3]. In view of the dependence of k' on platelet size within one whole platelet population, it is possible that shifts in the distribution of platelet sizes would similarly alter average k' values measured for the whole population. For example, changes in megakaryocyte ploidy distribution favouring the production of large platelets would increase the average optical efficiency of the platelet population. Such deviations in platelet production may occur in response to thrombocytopenia and/or be associated with platelet disorders. Indeed, it has been suggested that optical efficiencies for disease-state platelets (e.g., Bernard-Soulier Syndrome, May-Hegglin and others) would be different from that of normals [5]. The difference in efficiency would be attributable to altered platelet size distribution and/or pathological properties. In light of the above considerations, platelet optical efficiency appears to be a parameter of platelet heterogeneity and may serve as a useful index in the diagnosis of platelet disorders.

Figure A. The dependence of platelet extinction (e) in plasma as a function of equivalent platelet surface area expressed as $v^{2/3}$. Extinction was measured in a Payton aggregometer for control and size-dependent platelet subpopulations obtained from counterflow centrifugation ($r=0.81$, $p< 0.05$), with mean volumes (v) determined with the resistive particle counter.

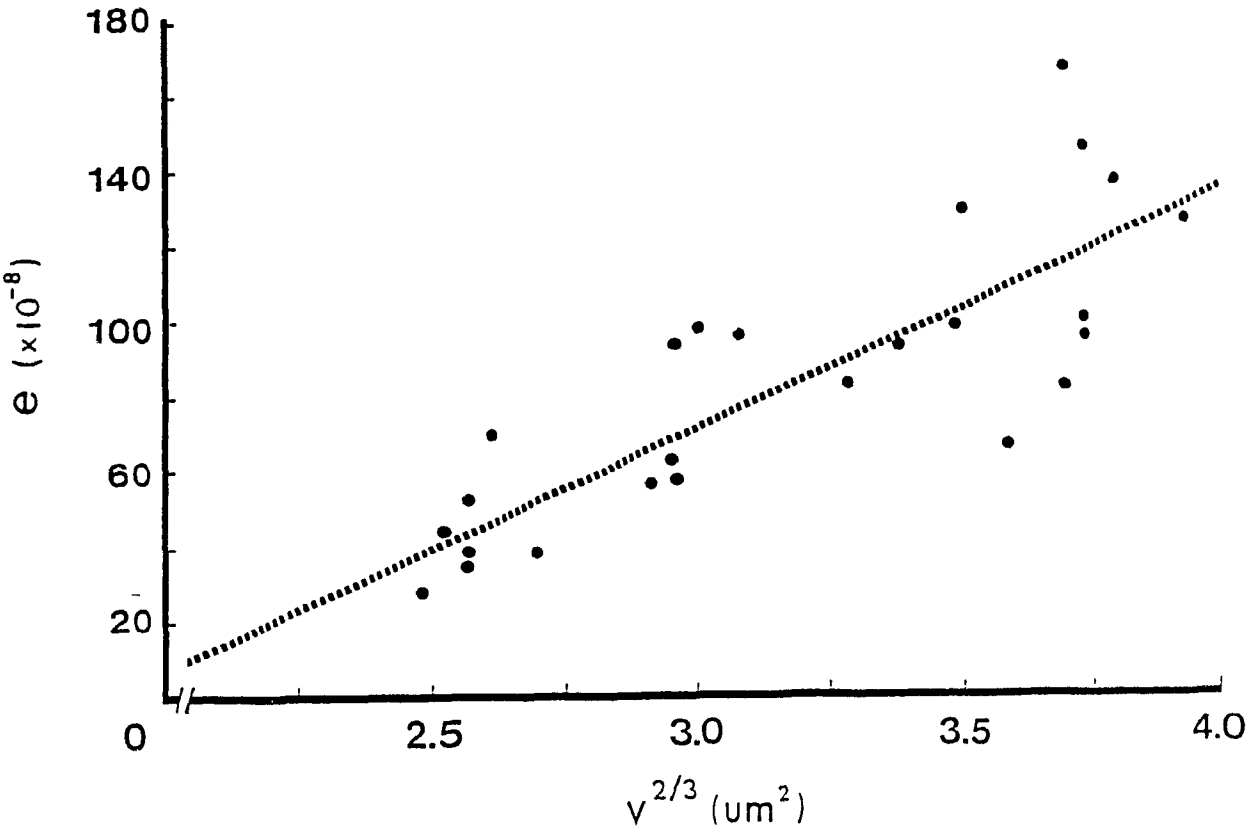

Table A: The relationship of optical extinction per unit area of platelet as a function of platelet size[a].

PLATELET FRACTION	SIZE		OPTICAL EFFICIENCY[c]	
	v (fl)	RELATIVE VALUES[b]	$\frac{e}{v^{2/3}}$ ($10^{-8}um^{-2}$)	RELATIVE VALUES[b]
L	7.3±0.2	1.8±0.2	32.3±8.2	1.9±0.2
M	5.6±0.6	1.3±0.2	25.3±7.6	1.5±0.2
S	4.1±0.2	1.0	16.9±5.1	1.0
C	6.1±0.2	1.4±0.2	27.7±1.4	1.6±0.2

[a]Number of donors: n=7 except for reconstituted control where n=4. Values are expressed as mean±S.D.

[b]Relative values to S platelets, i.e., L:S, M:S, and C:S. These ratios were calculated for each individual donor, and expressed as a mean±S.D. for the pooled donors.

[c]See equation 6 for the relation between $e/v^{2/3}$ and optical efficiency.

REFERENCES

1) Frojmovic M M. Rheooptical studies of platelet structure and function. Progr Hemost Thrombos 1978:4;279-319.

2) Frojmovic M M, Panjwani R. Blood cell structure-function studies:light transmissions and attenuation coefficients of suspensions of blood cells and model particles at rest and with stirring. J Lab Clin Med 1975:86;326-343.

3) Latimer P. Light scattering and absorption as methods of studying cell population parameters. Ann Rev Biophys Bioeng 1982:11;129-150.

4) Milton J G, Frojmovic M M. Turbidometric evaluations of platelet activation: relative contributions of measured shape change, volume, and early aggregation. J Pharm Methods 1983:9;101-115.

5) Holme S, Simmonds M, Ballek R, Murphy S. Comparative measurements of platelet size by Coulter Counter, microscopy of blood smears, and light transmission studies. J Lab Clin Med 1981:97;610-622.